# Physics & Quantum Computers at hiMolde

www.himolde.no

Molde University College

Per Kristian Rekdal, 31st August 2011

# Outline

- Presentation of myself
- My next 3 years at hiMolde
- Theoretical physics: Quantum Optics
- Quantum computers:
  - superposition
  - entanglement
- Decoherence
  - Lifetime of an atom chip (PRL 97, 070401 (2006) )
- Collaborators
- Summary

# Presentation

- Name: Per Kristian Rekdal
- Age: 38
- Education:
  - M. Sci.: theoretical physics, NTNU, (1992-1997)
  - Ph.D.: quantum optics, NTNU, (1998-2001)
  - Post Doc: quantum optics, Imperial C., (2002-2004)
  - Post Doc: quantum optics, UniGraz, (2005-2006)
- # published papers: 14
- h-index : 6

Molde University College
Specialized University in Logistics

# Presentation (cont.)

- **Master of Science**: (1992-1997)
  NTNU
  Thesis:
  *"Coherent Electron Transport in Two-Dimentional Quantum Dot-Structures in a Magnetic Field"*

  Supervisor: Eivind Hiis Hauge

Molde University College
Specialized University in Logistics

# Presentation (cont.)

- **Doctoral fellow**: (1997-2001)
  NTNU
  Dr. Ing. Thesis:
  *"Some Non-Perturbative Results in Modern Quantum Optics"*
  Supervisor: Prof. Bo-Sture Skagerstam

Molde University College
Specialized University in Logistics

# Presentation (cont.)

- **Doctoral fellow**: (1997-2001)
  NTNU
  Dr. Ing. Thesis:
  *"Some Non-Perturbative Results in Modern Quantum Optics"*
  Supervisor: Prof. Bo-Sture Skagerstam

Molde University College
Specialized University in Logistics

# Presentation (cont.)

- **Post doctoral fellow**: (2002-2004)
  Imperial College London, England
  Co-workers:
  Dr. S. Scheel, Prof. E. Hinds and Prof. P. Knight




Molde University College
Specialized University in Logistics

# Presentation (cont.)

- **Doctoral fellow**: (2005-2006)
  Karl-Franzens-Universitä Graz, (Austria)
  Co-workers:
  Ulrich Hohenester

Molde University College
Specialized University in Logistics

# Presentation (cont.)

Non-academic work experience:


- Axess A/S, Molde (2007-2011)
- Structural Engineer
  - analysis and calculation
  - FEM analysis
  - “hand calculation”
- IT responsible (2007-2010)
  - strategical decisions
  - some technical issues

## Structural Engineer, analysis and calculation, (2007-2011):

AXESS

| | | | | | | |
|---|---|---|---|---|---|---|
| Project: | Borgland Dolphin – Upgrade of Riser Handling Crane | | Project no.: | 1436 | | |
| Client: | Dolphin AS | Prepared | Date: 14.08.09 | Sign.: PKR | Doc. no.: 1436-250-01_02 | |
| Subjects: | Structural strength analysis | Verified | Date: 14.08.09 | Sign.: ONE | Rev.: 02 | Page / of: 28 / 50 |

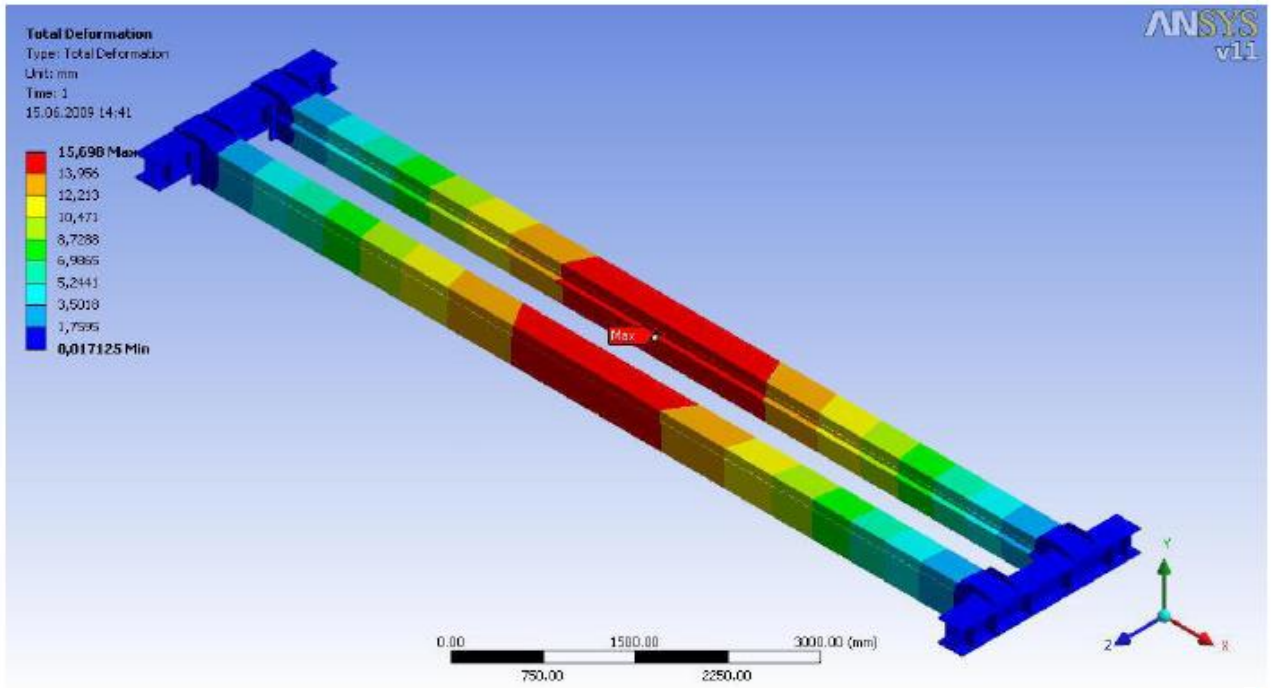


Figure 7-5: Deflection of bridge beam for load combination I. Max deflection is 15.6mm.

Molde University College
Specialized University in Logistics

## Structural Engineer, analysis and calculation, (2007-2011):

AXESS

| | | | | | | |
|---|---|---|---|---|---|---|
| Project: | Borgland Dolphin – Upgrade of Riser Handling Crane | | Project no.: | 1436 | | |
| Client: | Dolphin AS | Prepared | Date: 14.08.09 | Sign.: PKR | Doc. no.: 1436-250-01_02 | |
| Subjects: | Structural strength analysis | Verified | Date: 14.08.09 | Sign.: ONE | Rev.: 02 | Page / of: 18 / 50 |

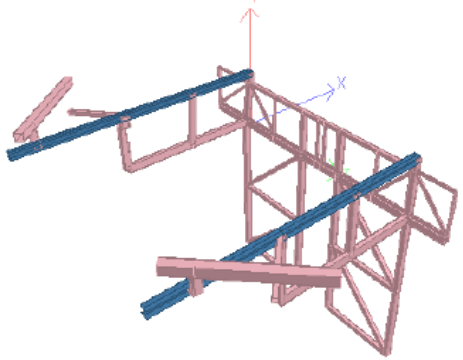

Figure 5-1: The structure as modelled in STAAD.Pro.

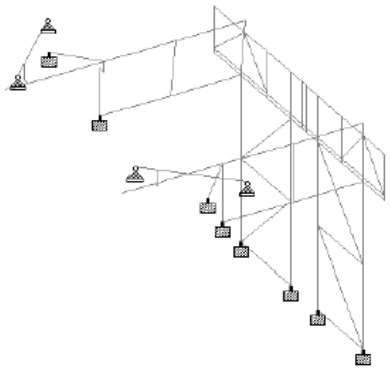

Figure 5-2: Eight nodes in the STAAD.Pro model are "fixed support". Four nodes are modelled with "pinned support".

Molde University College
Specialized University in Logistics

## Structural Engineer, analysis and calculation, (2007-2011):

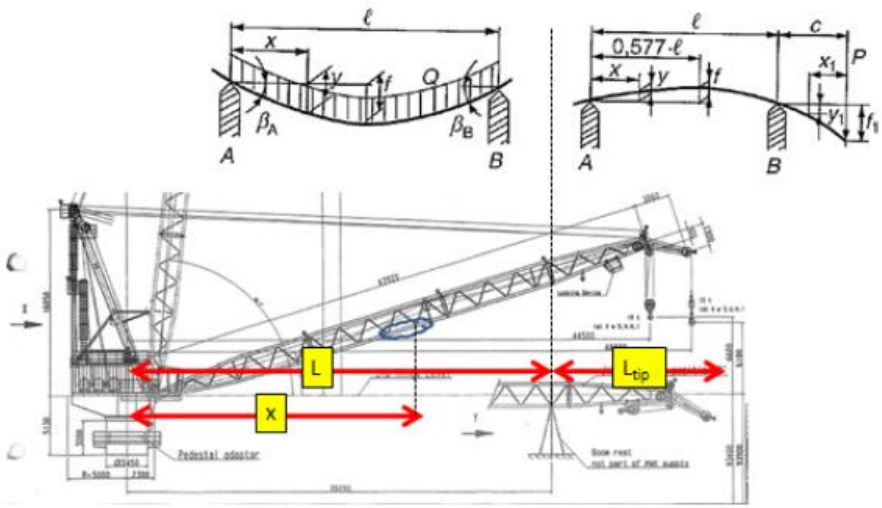


**Figure 2.1:** Model of boom for calculation.

$x := 22 \cdot m$ — position of damage, Ref.\R1\

$L := (34475 - 2300) \cdot mm = 32.175\,m$ — length of boom, Ref. drawing \D1\ ( see Fig. 2.1 )

$L_{tip} := (48000 - 36090) \cdot mm = 11.91\,m$ — length of boom tip, Ref. drawing \D1\ ( see Fig. 2.

$q := 500 \cdot \frac{kg}{m}$ — estimated weight of boom per meter (SolidWorks)

$Q := q \cdot L = 16.087 \cdot t$ — weight of boom between axle and boom rest

$Q_{tip} := q \cdot L_{tip} = 5.955\,t$ — weight of boom tip (see Fig. 2.1 )

$M := Q \cdot g \cdot \frac{x}{2} \cdot \left(1 - \frac{x}{L}\right) = 548.805 \cdot kNm$ — bending moment between king and boom rest

$M_{tip} := \frac{(Q_{tip} \cdot g) \cdot \frac{L_{tip}}{2} \cdot x}{L} = 237.787\,kNm$ — bending moment due to weighg of boom tip ( assume point load at $L_{tip}/2$ )

Molde University College
Specialized University in Logistics

# Presentation (cont.)

Present position:

- Associate Professor II at Molde University College ( “Førsteamanuensis II” )
- 20 % position
- Period: 3 years
- External funding
- Unit: Økonomi-, informatikk- og samfunnsfag (ØIS)

Molde University College
Specialized University in Logistics

# Next 3 years

Intentions for the next 3 years:

- 1) research and publication at hiMolde
  - "*Memory Effects in Spontaneous and Stimulated Emission Processes*"
  - "*Casimir Polder Force for an Atom above a superconductor at finite temperature T*"
  - "*Interference Effects for Emission Processes with Arbitrary Initial State*"
- 2) research collaboration with groups at hiMolde
  - e.g. optimization group (Arne Løkketangen)
- 3) teaching
  - MAT001 Forkurs i matematikk, 2011
  - Written a compendium

Molde University College
Specialized University in Logistics

# Next 3 years (cont.)

Paper currently under preparation:

## Memory Effects in Spontaneous and Stimulated Emission Processes

Asle Heide Vaskinn,[1,*] Arne Løhre Grimsmo,[1,†] Per Kristian Rekdal,[2,‡] and Bo-Sture Skagerstam[1,§]

[1] *Department of Physics, The Norwegian University of Science and Technology, N-7491 Trondheim, Norway*
[2] *Molde University College, P.O. Box 2110, N-6402 Molde, Norway*

(Dated: May 15, 2011)

We consider a quantum-mechanical analysis of a decaying systems in terms of an effective two-level system. The analysis is in principle exact, even though presented as a numerical solution of the time-evolution including memory effects, and is confronted with previous results as discussed in the literature in terms of e.g. approximative Laplace transform techniques. At large times as compared to the life-time of spontaneous emission we find large deviations of the exact analysis. We argue that different renormalization procedure actually influences the large-time behaviour of the decaying system. In the presence of physical boundaries the conclusions remains the same (?)

PACS numbers: 34.35.+a, 03.65.Yz, 03.75.Be, 42.50.Ct

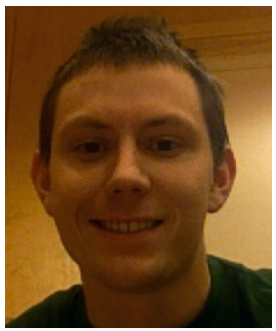


# Next 3 years (cont.)

## Memory Effects in Spontaneous and Stimulated Emission Processes

Asle Heide Vaskinn,[1,*] Arne Løhre Grimsmo,[1,†] Per Kristian Rekdal,[2,‡] and Bo-Sture Skagerstam[1,§]

[1] *Department of Physics, The Norwegian University of Science and Technology, N-7491 Trondheim, Norway*
[2] *Molde University College, P.O. Box 2110, N-6402 Molde, Norway*

(Dated: May 15, 2011)

We consider a quantum-mechanical analysis of a decaying systems in terms of an effective two-level system. The analysis is in principle exact, even though presented as a numerical solution of the time-evolution including memory effects, and is confronted with previous results as discussed in the literature in terms of e.g. approximative Laplace transform techniques. At large times as compared to the life-time of spontaneous emission we find large deviations of the exact analysis. We argue that different renormalization procedure actually influences the large-time behaviour of the decaying system. In the presence of physical boundaries the conclusions remains the same (?)

PACS numbers: 34.35.+a, 03.65.Yz, 03.75.Be, 42.50.Ct

### I. INTRODUCTION

The development concerning the manipulation of single atoms and their interaction with the electro-magnetic field has reached an impressive state of the in recent years (see e.g. Refs. [1–3]). Experimental studies have e.g. shown that artificial atoms can lead to a Lamb shift of the order of a few procent of the typical emission line [4]. Rather old issues concerning necessary deviations from exponential decay [5–15] may therefore be confronted with our current theoretical experimental understanding of decaying quantum systems. Concerning experimental studies of deviations from the conventional exponential decay we notice the study of decaying $\tau$-leptons [16], the observed deviations in quantum-mechanical tunneling processes [17] and the power-low behaviour of the decay at times-scales larger than twenty life-times in dissolved organic materials [18]. In nuclear physics the decay of thorium has also been suggested as a potential target for large-time deviations [19].

In the context elementary particle physics gauge invariant definitions of observable quantities are of importance and the definition of a the decay width of an unstable particle is highly non-trivial (see e.g. [20]) in this respect. In studies of a possible proton decay in Nature the time-dependence of decaying systems may also play an important role [21].

The paper is organized as follows. In the next section we outline the theoretical framework. In order to obtain ...

*Electronic address: asle.vaskinn@ntnu.no
†Electronic address: arne.grimsmo@ntnu.no
‡Electronic address: per.k.rekdal@himolde.no
§Electronic address: bo-sture.skagerstam@ntnu.no

### II. GENERAL THEORY

Let us consider a neutral atom at a fixed position $\mathbf{r}_A$. We will consider, in order to be specific, hyper-fine interactions but the results obtained can easily be rephrased in terms of eletric-dipole interactions. The magnetic moment of the atom interacts with the quantized magnetic field via a conventional Zeeman coupling. The total, unrenormalized, Hamiltonian is then the standard form

$$H = \sum_\alpha \hbar\omega_\alpha |\alpha\rangle\langle\alpha| + \int d^3r \int_0^\infty d\omega\, \hbar\omega\, \hat{\mathbf{f}}^\dagger(\mathbf{r},\omega)\cdot\hat{\mathbf{f}}(\mathbf{r},\omega) + H' \,, \quad (1)$$

where the effective interaction part is

$$H' = -\sum_\alpha\sum_\beta |\alpha\rangle\langle\beta|\, \boldsymbol{\mu}_{\alpha\beta}\cdot\mathbf{B}(\mathbf{r}_A) \,. \quad (2)$$

Here $\hat{\mathbf{f}}(\mathbf{r},\omega)$ is an annihilation operator for the quantized magnetic field, $|\alpha\rangle$ denotes the atomic state and $E_\alpha$ is the corresponding energy. We assume non-degenerate states, i.e. $E_\alpha \neq E_\beta$ for $\alpha \neq \beta$. The magnetic moment of the atom is $\boldsymbol{\mu}_{\alpha\beta} = \langle\alpha|\hat{\boldsymbol{\mu}}|\beta\rangle$, where $\hat{\boldsymbol{\mu}}$ is the magnetic moment operator. The magnetic field $\mathbf{B}(\mathbf{r}) = \mathbf{B}^{(+)}(\mathbf{r}) + \mathbf{B}^{(-)}(\mathbf{r})$ is written $\mathbf{B}^{(+)}(\mathbf{r}) = \nabla\times\mathbf{A}^{(+)}(\mathbf{r})$, where $\mathbf{B}^{(-)}(\mathbf{r}) = (\mathbf{B}^{(+)}(\mathbf{r}))^\dagger$ and where the vector potential is

$$\mathbf{A}^{(+)}(\mathbf{r}) = \mu_0 \int_0^\infty d\omega' \int d^3r'\, \omega' \sqrt{\frac{\hbar\epsilon_0}{\pi}\epsilon_2(\mathbf{r}',\omega')} \times \mathbf{G}(\mathbf{r},\mathbf{r}',\omega')\cdot\hat{\mathbf{f}}(\mathbf{r}',\omega') \,. \quad (3)$$

Here the imaginary part of the complex permittivity is $\epsilon_2(\mathbf{r},\omega)$. The dyadic Green tensor $\mathbf{G}(\mathbf{r},\mathbf{r}',\omega)$ is the unique solution to the Helmholtz equation

$$\overline{\nabla}\times\overline{\nabla}\times\boldsymbol{G}(\mathbf{r},\mathbf{r}',\omega) - \frac{\omega^2}{c^2}\epsilon(\mathbf{r},\omega)\boldsymbol{G}(\mathbf{r},\mathbf{r}',\omega) = \delta(\mathbf{r}-\mathbf{r}')\mathbf{1} \,, \quad (4)$$

Molde University College
Specialized University in Logistics

# Next 3 years (cont.)

where the arrow in $\overrightarrow{\nabla}$ denotes a derivation with respect to the first argument in the dyadic Greens function. Since the Helmholtz equation is a linear differential equation, the associated Green's tensor can be written as a sum according to

$$\mathbf{G}(\mathbf{r},\mathbf{r}',\omega) = \mathbf{G}^0(\mathbf{r},\mathbf{r}',\omega) + \mathbf{G}^S(\mathbf{r},\mathbf{r}',\omega)\,, \tag{5}$$

where $\boldsymbol{G}^0(\mathbf{r},\mathbf{r}',\omega)$ represents the contribution of the direct waves from the radiation sources in an unbounded medium, which is vacuum in our case, and $\boldsymbol{G}^S(\mathbf{r},\mathbf{r}',\omega)$ describes the scattering contribution of multiple reflection waves from the body under consideration. The presence of the vacuum part $\boldsymbol{G}^0(\mathbf{r},\mathbf{r}',\omega)$ in Eq.(5) will in general give rise to divergences in the energy shifts to be calculated below. A renormalization prescription is therefore required. We subtract the vacuum part $\boldsymbol{G}^0(\mathbf{r},\mathbf{r}',\omega)$, i.e. we neglect possible finite corrections due to this vacuum subtraction like conventional vacuum-induced Lamb shifts. Since we, in the end, are going to consider CP forces all additive coordinate independent corrections to energy shifts will, anyway, not contribute. When we below refer to a renormalization prescription the procedure above is what we then have in mind.

For reason of simplicity, we now limited our attention to a two-level atom approximation, i.e. an atom with an excited state and a ground state with the frequency transition $\omega_A \equiv (E_e - E_g)/\hbar > 0$. We consider the Hamiltonian in Eq.(1) and apply the well-known Weisskopf-Wigner theory for the transitions $e \to g$. The solution to the time-dependent Schrödinger equation in the rotating-wave approximation (RWA), i.e. applying $H' \approx H_{RWA}$, where

$$H_{RWA} = -|e\rangle\langle g|\,\boldsymbol{\mu}_{eg}\cdot\mathbf{B}^{(+)}(\mathbf{r}_A) + \text{h.c.}\,, \tag{6}$$

is then ($\omega_e \equiv E_g/\hbar$)

$$\begin{aligned}|\psi(t)\rangle &= c_e(t)\,e^{-i\omega_e t}\,|e\rangle\otimes|0\rangle \\ &+ \int d^3r \int_0^\infty d\omega \sum_{m=1}^{3} \\ &\times\; c_g(\mathbf{r},\omega,m|t)\,e^{-i(\omega+\omega_g)t}|g\rangle\otimes|\mathbf{r},\omega,m\rangle\,,\end{aligned} \tag{7}$$

as we have ignored any higher order photon state than the 0-photon and 1-photon state. Here $|e\rangle$ and $|g\rangle$ are the excited state and ground state for the atom, respectively. Furthermore, $|0\rangle$ denotes the vacuum of the electro-magnetic field and $|\mathbf{r},\omega,m\rangle = \hat{f}^\dagger_m(\mathbf{r},\omega)\,|0\rangle$ is a one photon state. The probability amplitudes $c_e(t)$ and $c_g(\mathbf{r},\omega,m|t)$ must then obey the unitarity condition

$$|c_e(t)|^2 + \int d^3r \int_0^\infty d\omega \sum_{m=1}^{3} |c_g(\mathbf{r},\omega,m|t)|^2 = 1\,. \tag{8}$$

In the present paper we will restrict ourselves to the initial conditions $c_e(0) = 1$ and $c_g(\mathbf{r},\omega,m|t=0) = 0$ and consider more general initial conditions elsewhere. The probability amplitude for the excited atomic state $c_e(t)$ is then determined by (see e.g. Refs.[22, 23])

$$\dot{c}_e(t) \;=\; \int_0^t dt'\,K(t-t')\,c_e(t')\,, \tag{9}$$

where the kernel $K(t)$ is

$$K(t) \;=\; -\frac{1}{2\,\pi}\int_0^\infty d\omega\, e^{-i(\omega-\omega_A)t}\Gamma(\mathbf{r}_A,\omega)\;. \tag{10}$$

Here we have made use of the conventional spin-flip decay rate for spontaneous emission as given by

$$\Gamma(\mathbf{r},\omega) = \frac{2\,\mu_0}{\hbar}\boldsymbol{\mu}_{eg}\cdot\mathrm{Im}[\overrightarrow{\nabla}\times\mathbf{G}(\mathbf{r},\mathbf{r},\omega)\times\overleftarrow{\nabla}]\cdot\boldsymbol{\mu}_{ge}\,, \tag{11}$$

where the arrow in $\overleftarrow{\nabla}$ now denotes a derivation with respect to the second argument in the dyadic Greens function. We also have that

$$\begin{aligned}&c_g(\mathbf{r},\omega,m|t) = \\ &\frac{i}{e}\sqrt{\frac{\mu_0}{\hbar}}(\boldsymbol{\mu}^*_{ge}\cdot(\overrightarrow{\nabla}\times\mathbf{G}^*(\mathbf{r}',\mathbf{r},\omega)|_{\mathbf{r}'=\mathbf{r}_A}))_m I(\omega-\omega_A,t)\,,\end{aligned} \tag{12}$$

where

$$I(\omega,t) = \int_0^t dt' e^{i\omega t'} c_e(t')\,. \tag{13}$$

The useful identity

$$\int d^3r \frac{\omega^2}{c^2}\varepsilon_I(\mathbf{r},\omega)G_{jm}(\mathbf{r}',\mathbf{r})G_{lm}(\mathbf{r}'',\mathbf{r}) = \mathrm{Im}G_{jl}(\mathbf{r}',\mathbf{r}'')\,, \tag{14}$$

and Eq.(12) now leads to

$$\begin{aligned}&\int d^3r \int_0^\infty d\omega \sum_{m=1}^{3} |c_g(\mathbf{r},\omega,m|t)|^2 = \\ &\frac{1}{2\pi}\int_0^\infty d\omega\,\Gamma(\mathbf{r_A},\omega)|I(\omega-\omega_A,t)|^2\,.\end{aligned} \tag{15}$$

It now follows from Eqs.(9) and (15) that

$$\frac{d}{dt}\left(|c_e(t)|^2 + \int d^3r \int_0^\infty d\omega \sum_{m=1}^{3} |c_g(\mathbf{r},\omega,m|t)|^2\right) = 0\,, \tag{16}$$

i.e. the unitarity condition Eq.(8) is fulfilled for all times as it should.

Eq.(9), a well-known Volterra integral equation of second kind, may be integrated with respect to time. The result is then

$$c_e(t) = 1 + \int_0^t dt'\,\kappa(t-t')\,c_e(t')\,, \tag{17}$$

Molde University College
Specialized University in Logistics

# Next 3 years (cont.)

where $\kappa(t) \equiv \int_0^t dt' K(t')$ is the integrated kernel, i.e.

$$\kappa(t) = \frac{1}{2\pi}\int_0^\infty d\omega \frac{e^{-i(\omega-\omega_A)t}-1}{i(\omega-\omega_A)}\Gamma(\mathbf{r}_A,\omega). \quad (18)$$

By passing, we mention that a rate similar to Eq.(11) may be derived for electric dipole transitions ( see e.g. Refs.[33, 34]). In that case, the spontaneous decay rate $\Gamma(\mathbf{r},\omega)$ should be replaced by

$$\Gamma_E(\mathbf{r},\omega) = \frac{2\,\omega_A^2}{\hbar\,\epsilon_0\,c^2}\,\boldsymbol{d}_{eg}\cdot \mathrm{Im}[\mathbf{G}(\mathbf{r},\mathbf{r},\omega)]\cdot\boldsymbol{d}_{ge}\,, \quad (19)$$

where $\boldsymbol{d}_{eg}$ is the electric dipole moment for the transition $e \to g$.

## III. VACUUM

### A. Exact

The Green tensor for vacuum is (see e.g. Refs.[23, 24])

$$\mathrm{Im}[\overleftarrow{\nabla}\times\mathbf{G}^0(\mathbf{r},\mathbf{r},\omega)\times\overrightarrow{\nabla}] = \frac{\omega^3}{6\pi\,c^3}\begin{bmatrix}1&0&0\\0&1&0\\0&0&1\end{bmatrix}. \quad (20)$$

In this case, the kernel for vacuum $\kappa_0(t)$ reads (c.f. Eq.(18))

$$\kappa_0(t) = \frac{\Gamma_0}{2\pi}\int_0^\infty d\omega\,\frac{\omega^3}{\omega_A^3}\,\frac{e^{-i(\omega-\omega_A)t}-1}{i(\omega-\omega_A)}. \quad (21)$$

Following Ref.[24], we restrict our attention to a two-level atom with no angular momentum and negligible nuclear moment. The decay rate of magnetic spin-flip transition for such an atom in free space is then (see also Refs.[34])

$$\Gamma_0 = \bar{\Gamma}_0 S^2\,, \quad (22)$$

with

$$\bar{\Gamma}_0 = \mu_0\,\frac{(\mu_B g_S)^2}{3\pi\,\hbar}\,k_A^3\,, \quad (23)$$

and $k_A \equiv \omega_A/c$ is the wave number in vacuum. Here we have introduced the dimensionless spin factor $S^2 \equiv S_x^2+S_y^2+S_z^2$, where $S_j \equiv \langle g|\hat{S}_j/\hbar|e\rangle$ is the dimensionless component of the electron spin operators $\hat{S}_j$ corresponding to the transition $|e\rangle \to |g\rangle$, with $j = x, y, z$. Furthermore, $\mu_B$ is the Bohr magneton, $g_S \approx 2$ is the electron spin $g$ factor.

Clearly, the kernel in Eq.(21) is divergent. As the case for magnetic dipole transition is analogue to the electric transition, we follow the same argument as far as renormalization concerns, i.e. applying Bethe's mass renormalization [36]. In the electric case, the kernel is renormalized such that the energy shift is reduced to a logarithmic divergence in the frequency $\omega$. Following this idea in the present magnetic case, we subtract the second order expansion of the denominator in Eq.(18) for $\omega \gg \omega_A$, i.e.

$$\frac{1}{\omega-\omega_A} \to \frac{1}{\omega-\omega_A} - \left(\frac{1}{\omega}+\frac{\omega_A}{\omega^2}+\frac{\omega_A^2}{\omega^3}\right), \quad (24)$$

which leaves us with the following renormalized version of the kernel Eq.(21):

$$\kappa_0^R(t) = \frac{\Gamma_0}{2\pi}\int_0^{\omega_c} d\omega\,\frac{e^{-i(\omega-\omega_A)t}-1}{i(\omega-\omega_A)}. \quad (25)$$

Here we have introduced a cut-off frequency $\omega_c$ in order to make the frequency integral should be finite. Since our calculation is non-relativistic we identify this cut-off with with $m_e c^2/\hbar$ and we introduce a dimensionless parameter is

$$\Lambda \equiv \frac{m_e c^2}{\hbar\omega_A}. \quad (26)$$

This renormalization procedure enables us to extract the leading logarithmic dependence of the cut-off parameter $\Lambda$ in the renormalized kernel, i.e.

$$\kappa_0^R(t) = -\frac{\Gamma_0}{2\pi}\int_{-\omega_A}^{(\Lambda-1)\omega_A} dx\,\frac{\sin(xt)}{x} - i\frac{\Gamma_0}{2\pi}\int_{\omega_A}^{(\Lambda-1)\omega_A} dx\,\frac{\cos(xt)}{x} + i\frac{\Gamma_0}{2\pi}\ln(\Lambda-1). \quad (27)$$

The imaginary logarithmic term in this equation corresponds to a Lamb shift which therefore can be removed by introducing the energy shift

$$\tilde{\omega}_A \equiv \omega_A - \frac{\Gamma_0}{2\pi}\ln(\Lambda-1)\,, \quad (28)$$

and applying the transformation

$$c_e(t) \to \tilde{c}_e(t) \equiv c_e(t)\,\exp\left[-i\frac{\Gamma_0 t}{2\pi}\ln(\Lambda-1)\right]. \quad (29)$$

We also define a kernel

$$\tilde{\kappa}_0^R(t) = -\frac{\Gamma_0}{2\pi}\left[\mathrm{Si}[(\Lambda-1)\tilde{\omega}_A t]+\mathrm{Si}[\tilde{\omega}_A t]\right] - i\frac{\Gamma_0}{2\pi}\left[\mathrm{Ci}[(\Lambda-1)\tilde{\omega}_A t]-\mathrm{Ci}[\tilde{\omega}_A t]\right], \quad (30)$$

where $\mathrm{Ci}(x)$ and $\mathrm{Si}(x)$ are the Cosine and Sine integral, respectively (see e.g. Ref.[26]). The probability amplitude $\tilde{c}_e(t)$ is now a solution to the integral equation Eq.(17) provided the kernel $\kappa_0^R(t)$ is replaced by $\tilde{\kappa}_0^R(t)$. The solutions of the corresponding integral equation cannot be obtained in closed from and therefore we will resort to numerical considerations.

# Next 3 years (cont.)

### B. Approximations

It is convenient to define a dimensionless time parameter $\tau \equiv \Gamma_0 t$ as well as the parameter $\bar{b} \equiv \bar{\omega}_A/\Gamma_0$. Let us now consider small times $(\Lambda-1)\bar{b}\tau \ll 1$ and $\bar{b}\tau \ll 1$. Such small times are basically of academic interest as $t \ll \hbar/m_e c^2 = 1.2810^{-21}$ s. Virtual particles may then be created and our theory is not strictly valid. The leading series expansion of the kernel $\bar{\kappa}_0^R(t)$, as given by Eq.(30), for such small time parameters is:

$$\bar{\kappa}_0^R(\tau) \approx -\frac{\Gamma_0}{2\pi}\Lambda\,\bar{b}\tau - i\frac{\Gamma_0}{2\pi}\ln(\Lambda-1)\,. \qquad (31)$$

Apart from a sign, the imaginary part of this kernel is the same as the last imaginary part of Eq.(27). It is therefore convenient to invert the transformation Eq.(29) and consider the probability amplitude $c_e(\tau)$. Substituting the kernel $\bar{\kappa}_0^R(\tau)$ into Eq.(17), we obtain

$$c_e(\tau) \approx 1 - \frac{\Lambda}{4\pi\, b}(b\tau)^2\,, \qquad (32)$$

using the approximation $c_e(\tau') \approx 1$ in Eq.(17) since time is small. Notice that, in Eq.(32), it is the parameter $b \equiv \omega_A/\Gamma_0$ that enters and not the $\bar{b} \equiv \bar{\omega}_A/\Gamma_0$. In passing, we mention that an expansion for small times is also given in Ref.[31], with the result

$$c_e(\tau) \approx 1 - \frac{\Lambda^2}{8\pi}(b\tau)^2\,. \qquad (33)$$

The discrepancy between these last two expressions is easily explained by the fact that different renormalization procedures have been applied.

Let us still consider small times $\bar{b}\tau \ll 1$ but $(\Lambda-1)\bar{b}\tau \gg 1$. For such intermediate times, the kernel in Eq.(30) is reduced to

$$\bar{\kappa}_0^R(\tau) \approx -\frac{\Gamma_0}{4} + i\frac{\Gamma_0}{2\pi}[\,\gamma_E + \ln(\bar{b}\tau)\,]\,, \qquad (34)$$

where $\gamma_E \approx 0.577\,216$ is Euler's constant. Substituting Eq.(34) into the Eq.(17), expressed in terms of $\tilde{c}_e(\tau)$ and using $\tilde{c}_e(\tau') \approx 1$, we may then carry out the time integration, with the result

$$\tilde{c}_e(\tau) \approx 1 - \frac{\tau}{4} + i\frac{\tau}{2\pi}\left(\gamma_E + \ln(\bar{b}\tau) - 1\right)\,. \qquad (35)$$

The corresponding probability $|\tilde{c}_e(\tau)|^2 = |c_e(\tau)|^2$ is plotted in Fig.1 (dotted line) together with the exact numerical solution, i.e. the numerical solution of Eq.(17) with the exact kernel Eq.(30) (solid line).

Finally, for large times as compared to the shifted atomic frequency transition, i.e. $\bar{b}\tau \gg 1$, and also $(\Lambda-1)\bar{b}\tau \gg 1$, the kernel Eq.(30) is, to first leading order

$$\bar{\kappa}_0^R(\tau) \approx -\frac{\Gamma_0}{2} + \frac{\Gamma_0}{2\pi}\frac{e^{i\bar{b}\tau}}{\bar{b}\tau}\,. \qquad (36)$$

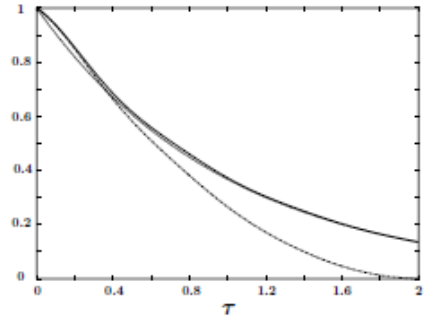


FIG. 1: The probability $|c_a(\tau)|^2 = |\tilde{c}_a(\tau)|^2$ as a function of $\tau \equiv \Gamma_0 t$. The solid line corresponds to the exact numerical solution, i.e. solution of Eq.(17) with the kernel Eq.(27) for a two-level system in vacuum. The dash-dotted line corresponds to the small-time expansion Eq.(35). The latter case is valid for $\bar{b}\tau \ll 1$. The dotted line corresponds to the exponential decay $\exp(-\tau)$ with expected deviations at small $\tau$. The values of the relevant parameters are $\bar{b} \equiv \bar{\omega}_A/\Gamma_0 = 10$ and $\Lambda = 1000$.

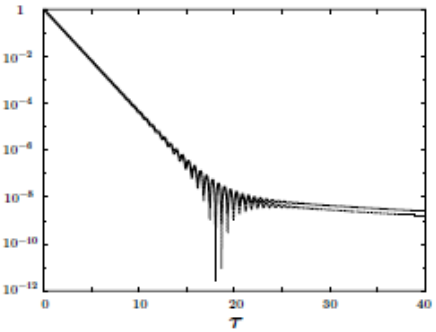


FIG. 2: The probability $|c_a(\tau)|^2 = |\tilde{c}_a(\tau)|^2$ as a function of $\tau \equiv \Gamma_0 t$. The solid line corresponds to the exact numerical solution, i.e. solution of Eq.(17) with the kernel Eq.(27) for a two-level system in vacuum. The dotted line corresponds to Eq.(37). The values of the relevant parameters are $\bar{b} \equiv \bar{\omega}_A/\Gamma_0 = 10$ and $\Lambda = 1000$.

This approximation serves as a motivation for the fitting formula

$$\tilde{c}_e(\tau) \approx e^{-\tau/2} + \frac{e^{i\bar{b}\tau}}{2\pi i\,\bar{b}(\bar{b}-1)\tau}\,. \qquad (37)$$

This solution includes the well-known exponential decay as well as a correction term. Eq.(37) is plotted in Fig. 2

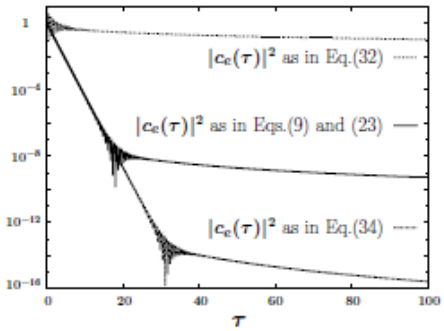


FIG. 3: The probability $|c_e(\tau)|^2$ as a function of $\tau \equiv \Gamma_0 t$. The solid line corresponds to the exact numerical solution, i.e. solution of Eq.(17) with the kernel Eq.(30) for a two-level system in vacuum. The dotted line corresponds to the main result in Ref.[29], i.e. Eq.(39), and the dashed-dotted line corresponds Eq.(41). The values of the relevant parameters are $c_e(0) = 1$, $b \equiv \omega_A/\Gamma_0 = 10$ and $\Lambda = 1000$. With these choices, $\tilde{b} \equiv \tilde{\omega}_A/\Gamma_0 = 9.65030$.

(dotted line) together with the exact numerical solution (solid line). The last term in Eq.(37) will dominate over the exponential for times $\tau \gtrsim \tau^\star$, where $\tau^\star$ is determined by the transcendental equation

$$e^{-\tau^\star/2} = \frac{1}{2\pi\,\tilde{b}(\tilde{b}-1)\tau^\star}\,. \tag{38}$$

For $\tilde{b} = 10$ as in Fig. 3, the solution of this equation is $\tau^\star \approx 18.5$.

### C. Comparison with Refs.[29, 31]

The subject concerning deviation from exponential decay for atomic spontaneous emission has been studied in the literature by several people (see e.g. Refs.[29]-[35]). In many cases, approximations have been applied in order to obtain analytical expressions for the expansion coefficient, as e.g. in Refs.[29, 31, 32]. In particular, several approximations have been applied by Knight and Milonni in Ref.[29], e.g. an equivalent to a rotation wave approximation, in order to obtain the following explicit expression for the probability amplitude:

$$c_e(\tau) = e^{-\tau/2} - \frac{e^{ib\tau}}{2\pi\,i} \times \int_0^\infty dx \left\{ \frac{e^{-\Lambda\,x\,b\tau}}{x - \frac{i}{\Lambda} + i\frac{x}{2b} - \frac{x}{2\pi\,b}\left[\ln x - i\frac{\pi}{2}\right]} + \frac{e^{-\Delta\,x\,\tau}}{x - \frac{i}{\Lambda} - \frac{x}{2\pi\,b}\left[\ln x + i\frac{\pi}{2}\right]} \right\}, \tag{39}$$

where $\Delta \equiv \delta\omega/\omega_A$ and

$$\delta\omega = \frac{\Gamma_0}{2\pi}\ln\Lambda\,, \tag{40}$$

is the 'energy shift' for the excited state $|e\rangle$. In this case, the initial condition is $c_e(0) = 1$. For large times, i.e. $b\tau \gg 1$, this expression is reduced to [29]

$$c_e(\tau) \;\approx\; e^{-\tau/2} + \frac{1}{2\pi\,b}\,\frac{1}{(b\tau)^2}\,e^{ib\tau}\,. \tag{41}$$

Notice the deviation between this equation and Eq.(37). For comparison, Eqs.(39) and (41) are plotted together with the exact numerical solution, see Fig.(3). We observe that, for small $\tau$, the absolute value of Eq.(39) is above unity. In addition, the asymptotic expression Eq.(41) seems to have wrong scaling in $\tau$ as compared to Eq.(39).

In Ref.[31], Seke and Herfort have considered the integral equation Eq.(17) for the vacuum case. The kernel applied in this case is analogous to Eq.(21), but with the integrand factor $\omega/\omega_A$ rather than $\omega^3/\omega_A^3$. The kernel may be written in terms of $\kappa_0^R(\tau)$ as given by Eq.(25):

$$\eta_0(\tau) = \kappa_0^R(\tau) + \frac{\Gamma_0}{2\pi b\tau}\left(e^{-i(\Lambda-1)b\tau} - e^{ib\tau}\right) + i\,\frac{\Gamma_0}{2\pi}\,\Lambda \tag{42}$$

In contrast $\kappa_0^R(\tau)$, the kernel $\eta_0(\tau)$ is linear in the dimensionless cut-off frequency rather logarithmic as in Eq.(27). The linear $\Lambda$-term may be absorbed in a energy shift such that the kernel may be written

$$\eta_0(\tau) \to \eta_0(\tau) = \kappa_0^R(\tau) + \frac{1}{2\pi\,b'\tau}\left(e^{-i(\Lambda-1)b'\tau} - e^{ib'\tau}\right) \tag{43}$$

where $b' \equiv \omega_A'/\Gamma_0$, and

$$\omega_A' \equiv \omega_A - \frac{\Gamma_0}{2\pi}\Lambda\,, \tag{44}$$

In Fig. 4 we have plotted the solution of Eq.(17) with the kernel Eq.(43). At least for $\tau \gtrsim \tau^\star$, the solution of Seke and Herfort has some addition oscillations.

## IV. ATOM NEAR A NON-MAGNETIC SLAB

Let us now consider the geometry semi-infinite non-magnetic slab with finite thickness, i.e. the same geometry as in Ref.[25] (Fig. 1). The components of the equal position dyadic Green tensor for such a slab is a diagonal matrix given by (see e.g. Ref.[25])

$$\overleftarrow{\nabla} \times \mathbf{G}^S(\mathbf{r},\mathbf{r},\omega) \times \overleftarrow{\nabla} = \frac{i}{4\pi}\begin{bmatrix} I_\parallel(\omega) & 0 & 0 \\ 0 & I_\parallel(\omega) & 0 \\ 0 & 0 & I_\perp(\omega) \end{bmatrix}\,, \tag{45}$$

# Next 3 years (cont.)



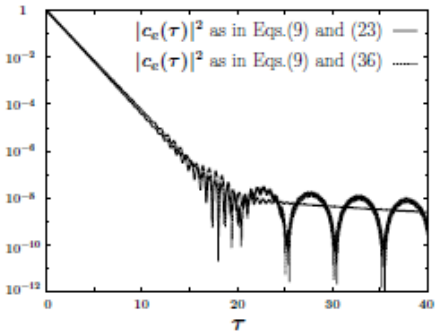


FIG. 4: The probability $|c_e(\tau)|^2$ as a function of $\tau \equiv \Gamma_0 t$. The solid line corresponds to the exact numerical solution, i.e. solution of Eq.(17) with the kernel Eq.(30) for a two-level system in vacuum. The dotted line corresponds to the solution of the Volterra equation as considered in Ref.[31], i.e. the solution of Eq.(17) with the kernel Eq.(43). The values of the relevant parameters are $c_e(0) = 1$, $\tilde{b} \equiv \tilde{\omega}_A/\Gamma_0 = 10$ and $\Lambda = 10$. With these choices, $b' \equiv \omega'_A/\Gamma_0 = 8.75815$.

where $\omega$ is real and $\overrightarrow{\nabla}$ indicates that the position derivative shall operate to the right. In the same fashion, $\overleftarrow{\nabla}$ means that the position derivative shall operate to the left. The elements of the matrix are the integrals

$$I_\parallel(\omega) = \frac{1}{2}\int_0^\infty d\lambda \frac{\lambda}{\eta_0(\lambda)} e^{i2\eta_0(\lambda)z} \times \left(\frac{\omega^2}{c^2} C_N(\lambda) - \eta_0^2(\lambda) C_M(\lambda)\right), \quad (46)$$

$$I_\perp(\omega) = \int_0^\infty d\lambda \frac{\lambda^3}{\eta_0(\lambda)} e^{i2\eta_0(\lambda)z} C_M(\lambda), \quad (47)$$

with the Fresnel coefficients

$$C_N(\lambda) = r_p(\lambda) \frac{1 - e^{i2\,\eta(\lambda)h}}{1 - r_p^2(\lambda) e^{i2\eta(\lambda)\,h}}, \quad (48)$$

$$C_M(\lambda) = r_s(\lambda) \frac{1 - e^{i2\eta(\lambda)\,h}}{1 - r_s^2(\lambda) e^{i2\eta(\lambda)\,h}}, \quad (49)$$

and

$$r_s(\lambda) = \frac{\eta_0(\lambda) - \eta(\lambda)}{\eta_0(\lambda) + \eta(\lambda)}, \quad (50)$$

$$r_p(\lambda) = \frac{\epsilon(\omega)\,\eta_0(\lambda) - \eta(\lambda)}{\epsilon(\omega)\,\eta_0(\lambda) + \eta(\lambda)}, \quad (51)$$

where $\eta(\lambda) = \sqrt{k^2\epsilon(\omega) - \lambda^2}$ and $\eta_0(\lambda) = \sqrt{k^2 - \lambda^2}$. The distance $h$ is the thickness of the slab, and $z \geq 0$ is the distance of the atom from the surface of the slab. The dielectric function is denoted $\epsilon(\omega)$. Both this function and the Green tensor are analytic in the upper half of the complex frequency plane.

## V. PERFECT CONDUCTING SLAB

The Volterra Eq.(17) for a two-level atom in the vicinity of a semi-infinite slab is hard to solve for a general dielectric function. Let us therefore consider a simpler special case, a perfect conductor, corresponding to the limit $\epsilon(\omega) \to \infty$ for all frequencies $\omega$. Strictly speaking, this limit is illegal as, for sufficiently large $\omega$, the dielectric function approaches $\epsilon(\omega)/\epsilon_0 \to 1$ and the Green tensor for the slab vanishes. Let us, however, assume that the perfect conductor limit may be performed before the frequency integrals are carried out, in which case we may apply the distributional identity

$$\int_0^\infty dk\, e^{\pm i\,kx} = \pi\,\delta(x) \pm i\,P\frac{1}{x}, \quad (52)$$

where $P$ indicates the principal value. Eq.(17) can then be written

$$c_e(t) - c_e(0) \approx \int_0^t dt'\,\kappa_0(t-t')\,c_e(t') + k_s \int_{2\frac{z}{c}}^t dt'\,c_e(t'-2\tfrac{z}{c}) + \int_0^t dt'\,\kappa_s(t-t')\,c_e(t'), \quad (53)$$

where

$$k_s \equiv i\frac{3}{8}\bar{\Gamma}_0\, e^{i\,2k_A z} \times \left[(S_x^2 + S_y^2)\frac{1}{2k_A z} + [S_z^2 + \frac{1}{2}(S_x^2 + S_y^2)]\frac{2(i\,2k_A z - 1)}{(2k_A z)^3}\right], \quad (54)$$

as well as $\kappa_s(t-t') \equiv \int_0^t dt_x\, K_s(t_x - t')$, and

$$K_s(t) = \frac{1}{8\pi^2}\frac{\mu_0}{\hbar}(\mu_B g_S)^2\, e^{i\omega_A t} \times \left\{ -[S_x^2 + S_y^2]\frac{(ik_A)^2}{2z} P_-(t) + [S_z^2 + \frac{1}{2}(S_x^2 + S_y^2)]\frac{2}{(2z)^3} \times [\,i\,2k_A z\,P_+(t) - P_-(t)\,]\right\}, \quad (55)$$

with

$$P_\pm(t) \equiv \frac{P}{t - \frac{2z}{c}} \pm \frac{1}{t + \frac{2z}{c}}. \quad (56)$$

The distance- and frequency parameter $k_s$, i.e. Eq.(54), corresponds to the contribution from the $\delta$-function in

# Next 3 years (cont.)

Eq.(52) and $K_s(t)$ in Eq.(55) corresponds to the principal value contribution.

In passing, we mention that the slab contribution in Eq.(53) originating from the $\delta$-function is consistent with causality. This fact is revealed by the argument in the coefficient $c_e(t-2z/c)$ and the lower limit $2z/c$ of the integral, i.e. no contribution from this term for small times $t < 2z/c$.

Eq.(54) may be re-written in the form

$$k_s = -\frac{1}{4}\Gamma_{\rm pc} - i\,\delta\omega_{\rm pc}\,, \tag{57}$$

where we have introduced

$$\frac{\Gamma_{\rm pc}}{\Gamma_0} \equiv \frac{3}{2}F_\parallel(k_A z)(S_x^2+S_y^2)+3F_\perp(k_A z)S_z^2\,, \tag{58}$$

$$\frac{\delta\omega_{\rm pc}}{\Gamma_0} \equiv \frac{1}{4}\left(\frac{3}{2}G_\parallel(k_A z)(S_x^2+S_y^2)+3G_\perp(k_A z)S_z^2\right), \tag{59}$$

and

$$F_\parallel(x) \equiv \frac{\sin(2x)}{2x} + F_\perp(x)\,, \tag{60}$$

$$F_\perp(x) \equiv \frac{2x\cos(2x)-\sin(2x)}{(2x)^3}\,, \tag{61}$$

$$G_\parallel(x) \equiv -\frac{\cos(2x)}{2x} + G_\perp(x)\,, \tag{62}$$

$$G_\perp(x) \equiv \frac{2x\sin(2x)+\cos(2x)}{(2x)^3}\,. \tag{63}$$

Writing $k_s$ in this fashion, we may easily compare its real part and imaginary parts with known results. If we ignore the vacuum term as well as the principal term in Eq.(53), we realize that the real part of $k_s$ corresponds to the decay rate and the imaginary part corresponds to the frequency shift. Actually, the term $\Gamma_{\rm pc}$ as given in Eq.(58) coincide exactly with the spin-flip rate for an atom above a perfectly conducting slab (see e.g. Eq.(20) in Ref.[37]).

For short distances (nonretarded limit) $k_A z \ll 1$, the parameter $k_s$ may be expanded, with the result (c.f. Eq.(57)):

$$\frac{\Gamma_{\rm pc}}{\Gamma_0} \approx S_x^2+S_y^2-S_z^2-\frac{2(k_A z)^2}{5}\left(2(S_x^2+S_y^2)-S_z^2\right) \tag{64}$$

$$\frac{\delta\omega_{\rm pc}}{\Gamma_0} \approx \frac{3}{64}\frac{S_x^2+S_y^2+2S_z^2}{(k_A z)^3}\,. \tag{65}$$

Notice that for the choice $S_x^2+S_y^2-S_z^2=0$, then $\Gamma_{\rm pc}/\Gamma_0 \to 0$ for $k_A z \to 0$. The imaginary part of $k_s$ in this limit, i.e. Eq.(65), is in exact agreement with the magnetic frequency shift (see e.g. Ref.[25]). In the opposite limit, i.e. long distance (retarded) limit $k_A z \gg 1$, Eq.(54) may be written

$$\frac{\Gamma_{\rm pc}}{\Gamma_0} \approx \frac{(S_x^2+S_y^2)\sin(2k_A z)}{8k_A z}+\frac{S_z^2\cos(2k_A z)}{16(k_A z)^2}\,, \tag{66}$$

$$\frac{\delta\omega_{\rm pc}}{\Gamma_0} \approx \frac{(S_x^2+S_y^2)\cos(2k_A z)}{8k_A z}-\frac{S_z^2\sin(2k_A z)}{16(k_A z)^2}\,. \tag{67}$$

From Eq.(66) we realize that the sign of $\Gamma_{\rm pc}$ depends on the choice of $k_A z$ in this limit. The imaginary part of $k_s$, i.e. Eq.(67), is not consistent with the frequency shift in Ref.[25] for large $k_A z$.

## VI. THE DRUDE MODEL

In vacuum, the Drude dispersion relation may be written (see e.g. Ref. [28])

$$\epsilon(\omega) = 1-\frac{\omega_p^2}{\omega(\omega+i\nu)}\,, \tag{68}$$

where for gold the plasma frequency is $\omega_p = 9.0$ eV and the relaxation frequency is $\nu = 35$ meV.

## VII. FINAL REMARKS

In addition to ...


## ACKNOWLEDGMENTS

This work has been supported in part by the Norwegian University of Science and Technology (NTNU) and the Norwegian Research Council (NFR). We acknowledge Reidar Rekdal for assistance in the numerical work.


## APPENDIX A: GREEN'S TENSOR FOR A SLAB

Her komme noe kasnkje.


[1] R. Folmana, P. Krügera, J. Schmidermayer, J. Denschlag, and C. Henkel and C. Zimmermann, "*Microscopic atom optics: From wires to an atom chip*", Adv. At., Mol., and Opt. Phys. **48**, 263 (2002).

# Next 3 years (cont.)


[2] *Atom Chips: Manipulating Atoms and Molecules with Microfabricated Structures*, special issue of Eur. Phys. J. D **35**, 1 (2006). Eds. C. Henkel, J. Schmiedmayer, and C. Westbrook.

[3] J. Fortágh and C. Zimmermann, "*Magnetic microtraps for ultracold atoms*", Rev. Mod. Phys. **79**, 235(2007).

[4] A. Fragner, M. Göppl, J. M. Fink, M. Baur, R. Bianchetti, P. J. Leek, A. Blais, and A. Wallraff, "*Resolving Vacuum Fluctuations in an Electrical Circuit by Measuring the Lamb Shift*", Science **322**, 1357 (2008).

[5] L. A. Khalfin "*Contribution to the Decay Theory of a Quasi-Stationary State* ", Sov. Phys. JETP **6**, 1053 (1958).

[6] L. P. Horwitz, J. A. LaVita, and J.-P. Marchand, "*The Inverse Decay Problem* ", J. Math. Phys. **12**, 2537 (1971).

[7] L. P. Horwitz, and J.-P. Marchand, "*The Decay-Scattering System* ", Rocky Mountain J. Math Phys. **1**, 225 (1974).

[8] P. Exner, "*Unstable Quantum Stable Systems and Feynman Integrals*", Sov. J. Nucl. Phys. **15**, 54 (1984).

[9] L. S. Schulman, "*Unstable Particles and the Poincaré Semigroup*", Ann. Phys. (N.Y.) **59**, 201 (1970).

[10] R. T. Robiscoe, and J. C. Hermanson, "*Exponential Decay With a Memory*", Am. J. Phys. **40**, 1443 (1972); *ibid.* **41**, 414 (1972).

[11] K. Sinha, "*On the Decay of an Unstable Particle*", Hel. Phys. Acta **45**, 619 (1972).

[12] J. Mostowski and K. Wódkiewski, "*On the Decay Law of Unstable States*", Bull. l'Acad. Pol. Sci. **21**, 1027 (1973).

[13] L. Fonda, G. C. Ghirardi, and A. Rimini, "*Decay theory of unstable quantum systems*", Rep. Prog. Phys. **41**, 587 (1978).

[14] H. Nakazato, M. Namiki and S. Pascazio "*Exponential Behaviour of a Quantum System in a Macroscopic Medium*", Phys. Rev. Lett. **73**, 1063 (1994).

[15] P. Facchi, H. Nakazato, and S. Pascazio "*From the Quantum Zeno to the Inverse Quantum Zeno Effect*", Phys. Rev. Lett. **86**, 2699 (2001).

[16] G. Alexander, J. Allison, N. Altekamp et al. "*Test of the Exponential Decay Law at Short Decay Times using Tau Leptons*", Phys. Lett. **368** , 244-250 (1996).

[17] S. R. Wilkinson, C. F. Bharucha, M.C. Fischer, K. W. Madison, P. R. Morrow, Q. Niu, B. Sundaram, and M. G. Raizen, "*Experimental Evidence for Non-Exponential Decay in Quantum Tunneling*", Nature **387**, 575 (1997).

[18] C. Rothe, S. I. Hintschich, and A. P. Monkman, "*Violation of the Exponential-Decay Law at Long Times*", Phys. Rev. Lett. **96**, 193601 (2006).

[19] A. M. Dykhne, and E. V. Tkalya, "$^{229m}Th(3/2^+, 3.5\ eV$ *and Check of the Exponentiality of the Decay Law*", JEPT Lett. **67**, 549 (1998).

[20] P. A. Grassi, B. A. Kniehl, and A. Sirlin "*Width and Partial Width of Unstable Particles*", Phys. Rev. Lett. **86**, 389 (2001).

[21] C. Bernardini, L. Maiani, and M. Testa "*Short-Time Behaviour of Unstable Systems in Field Theory and Proton Decay*", Phys. Rev. Lett. **71**, 2687 (1993).

[22] W. Vogel and D.G. Welsch, "*Quantum Optics*", Wiley-VCH, Third Ed. (Weinham, 2006)

[23] S. Scheel, L. Knöll, and D.G. Welsch, "*Spontaneous Decay of an Excited Atom in an Absorbing Dielectric*", Phys. Rev. A **60**, 4094 (1999).

[24] P.K. Rekdal, S. Scheel, P.L. Knight, and E.A. Hinds, "*Thermal Spin Flips in Atom Chips*", Phys. Rev. A **70**, 013811 (2004).

[25] B.-S. Skagerstam, P.K. Rekdal, and A.H. Vaskinn, "*Theory of Casimir-Polder Forces*", Phys. Rev. A **80**, 022902 (2009).

[26] "*Handbook of Mathematical Functions with Formulas, Graphs, and Mathematical Tables*", M. Abramowitz and I. Stegun, Washington, DC: National Bureau of Standards, 1970.

[27] M.P.A. Jones, C.J. Vale, D. Sahagun, B.V. Hall, and E.A. Hinds, "*Spin Coupling between Cold Atoms and the Thermal Fluctuations of a Metal Surface*", Phys. Rev. Lett. **91**, 080401 (2003).

[28] I. Brevik, J.B. Aarseth, J.S. Høye, and K.A. Milton, "*Temperature dependence of the Casimir effect*", Phys. Rev. E **71**, 056101 (2005).

[29] P.L. Knight, and P.W. Milonni, "*Long-Time Deviations from Exponential Decay in Atomic Spontaneous Emission Theory*", Phys. Lett. **56A**, 275 (1976).

[30] R.J. Cook, and P.W. Milonni, "*Quantum Theory of an Atom Near Partially Reflecting Walls*", Phys. Rev. A **35**, 5081 (1987).

[31] J. Seke, and W.N. Herfort, "*Deviations From Exponential Decay in the Case of Spontaneous Emission From a Two-Level Atom*", Phys. Rev. A **38**, 833 (1988).

[32] J. Seke, and W.N. Herfort, "*Finite-Time Deviations From Exponential Decay in the Case of Spontaneous Emission From a Two-Level Hydrogenic Atom*", Ed. J. Perina , Wiley, N.Y. 2001.

[33] L. Knöll, S. Scheel, and D.-G. Welsch, "*QED in Dispersing and Absorbing Media*", in "*Coherence and Statistics of Photons and Atoms*", Ed. J. Perina, Wiley, New York, 2001.

[34] H.T. Dung, L. Knöll, D.-G. Welsch, "*Spontaneous decay in the presence of dispersing and absorbing bodies: General theory and applications to spherical cavity*", Phys. Rev. A **62**, 053804 (2000).

[35] H.T. Dung, L. Knöll, D.-G. Welsch, "*van der Waals interaction and spontaneous decay of an excited atom ni a superlens-type geomtry*", Phys. Rev. A **78**, 053828 (2008).

[36] H.A. Bethe, Phys. Rev. **72**, 8399 (1947).

[37] P.K. Rekdal and B.-S. Skagerstam, "*Decay processes in the presence of thin superconducting films*", Phys. Rev. A **75**, 022904 (2007).

[38] W. Vogel and D.-G. Welsch, "*Quantum Optics*", 3rd ed. (Wiley-VCH, New York, 2006).

[39] C. Henkel, S. Pötting, and M. Wilkens "*Loss and heating of particles in small and noisy traps*", Appl. Phys. B **69**, 379-387 (1999).


Molde University College
Specialized University in Logistics

# Next 3 years (cont.)

# KOMPENDIUM

***FAG/KURS:***

**MAT001**
**FORKURS I MATEMATIKK**

***TITTEL:***

**Utvalgte grunnleggende emner i matematikk**

***FAG/KURSANSVARLIG:***

**Per Kristian Rekdal**

***FORFATTER(E):***

**Per Kristian Rekdal**

***Semester:***

**H 2011**



Høgskolen i Molde
Vitenskapelig høgskole i logistikk
Avdeling for Økonomi, Informatikk,
Samfunnsfag og Helse og Sosialfag

Molde University College
Specialized University in Logistics

Eksempel: ( 2. gradsligning med parameter $a$ )

$$x^2 - 2x + a = 0 \tag{1.275}$$

$$x = \frac{-(-2) \pm \sqrt{(-2)^2 - 4 \cdot 1 \cdot a}}{2 \cdot 1} = \frac{2 \pm \sqrt{4(1-a)}}{2} = 1 \pm \sqrt{1-a} \tag{1.276}$$

Vi må skille mellom $a = 1$, $a < 1$ og $a > 1$:

$$x = \begin{cases} 1 & , \text{ når } a = 1 \quad \text{(kun en løsning)} \\ 1 \pm \sqrt{1-a} & , \text{ når } a < 1 \quad \text{(to løsninger)} \\ \varnothing & , \text{ når } a > 1 \quad \text{(ingen løsning)} \end{cases} \tag{1.277}$$

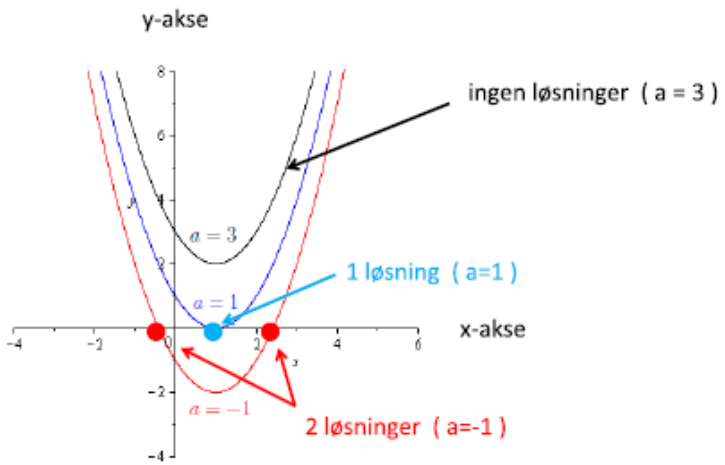


Figure 1.8: Plott av parabelen $f(x) = x^2 - 2x + a$ for $a = -1$, $a = 1$ and $a = 3$.

# Research

Field of research: Quantum Optics

Quantum Optics: (definition)

a field of research in physics, dealing with the application of quantum mechanics to phenomena involving light and its interactions with matter.

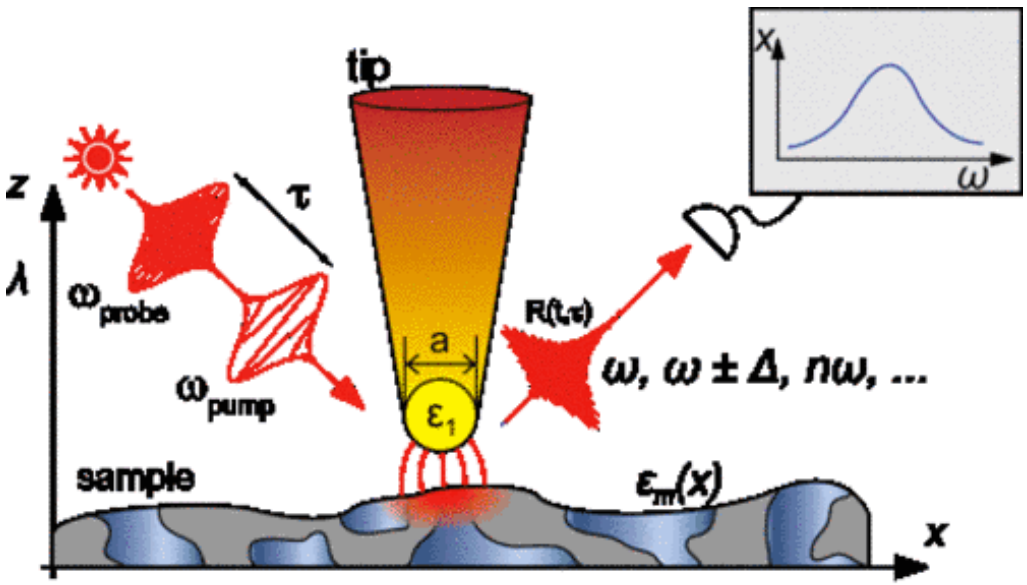

# Quantum Optics

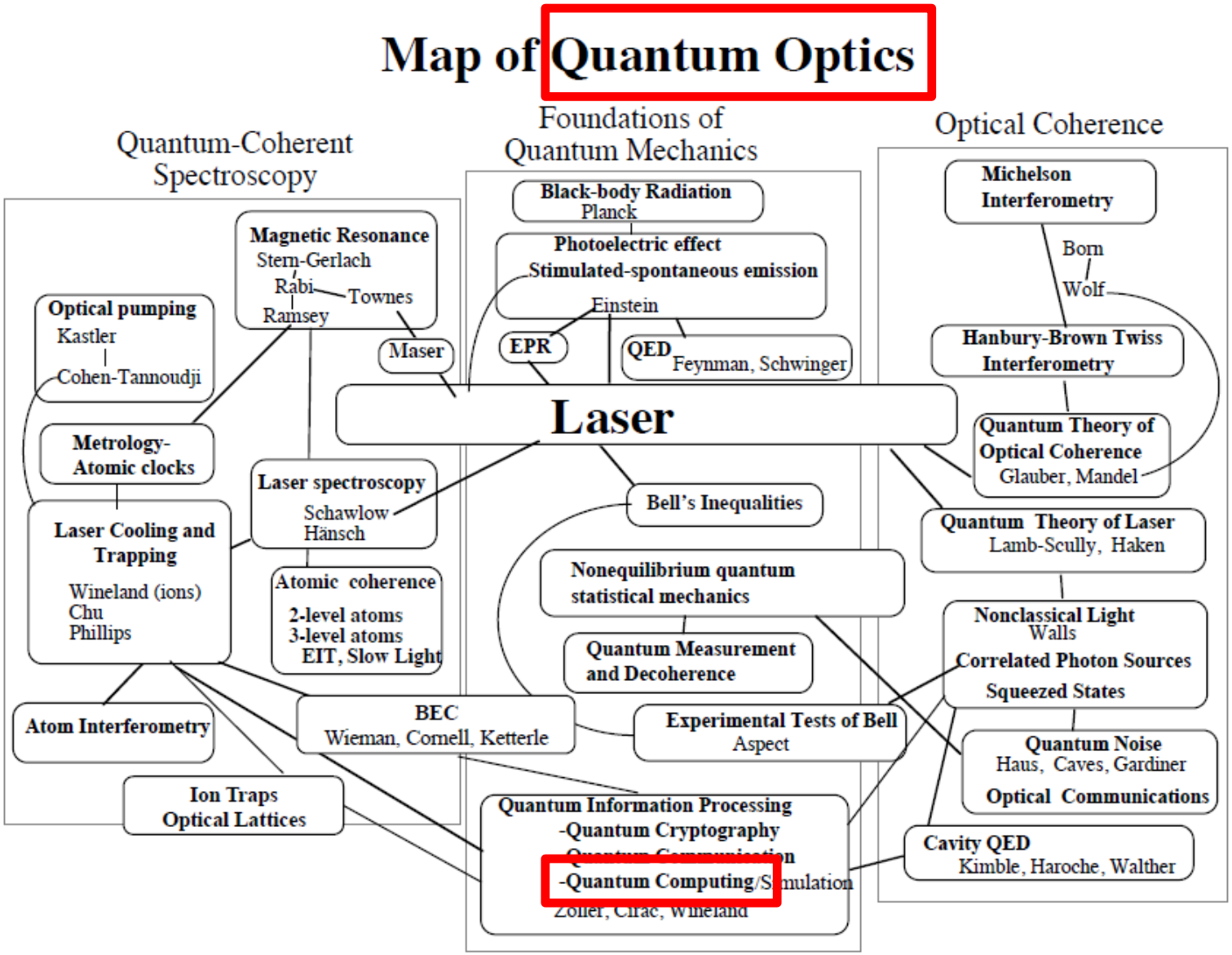

# Physics of computing

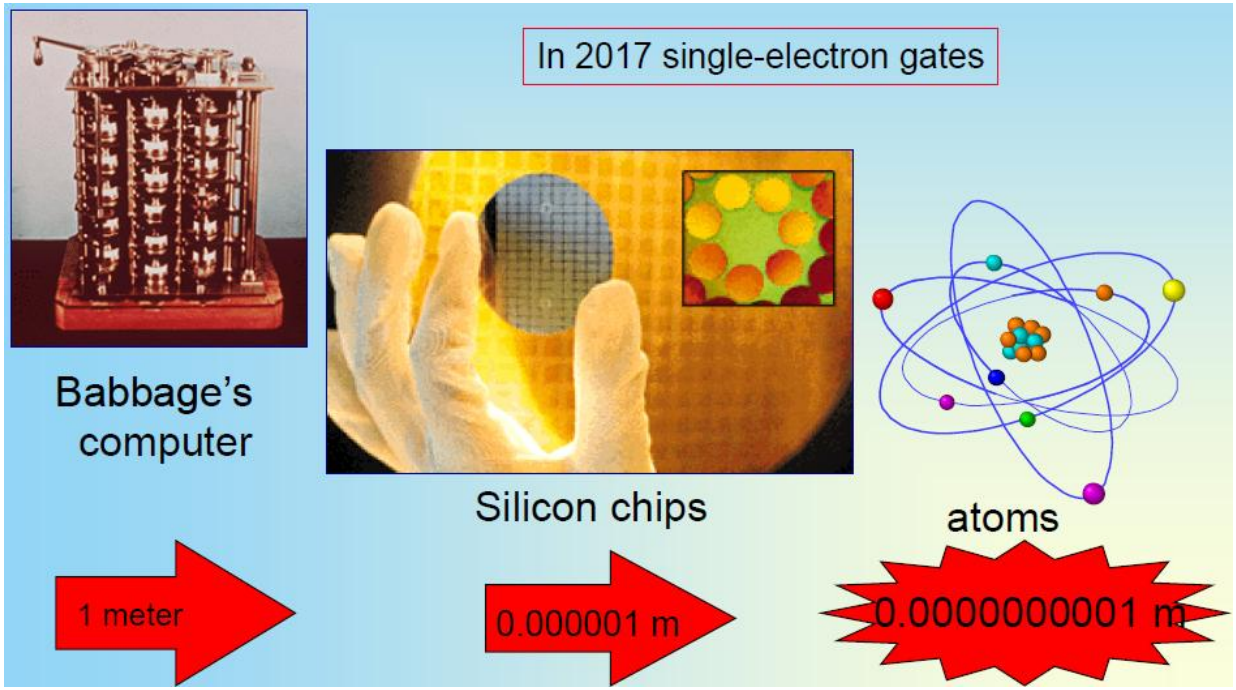


- Classical computer vs quantum computer:
  mechanical/circuits/transistors vs *atoms*
  ( bit vs qubit )

Molde University College
Specialized University in Logistics

# Bit vs Qubit

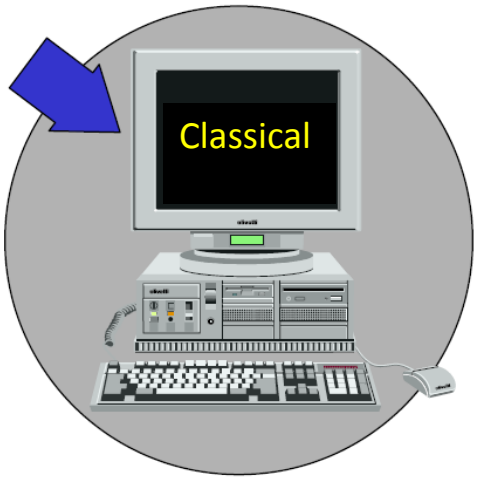


V
(voltage)

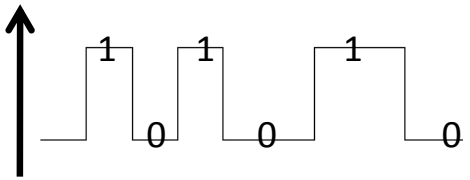


(electric)

**BIT**

(classical)

0 OR 1

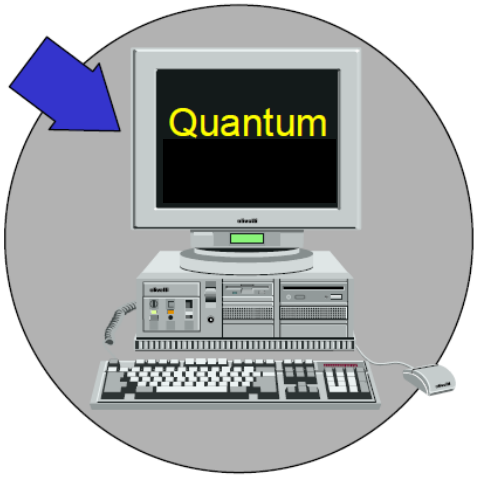


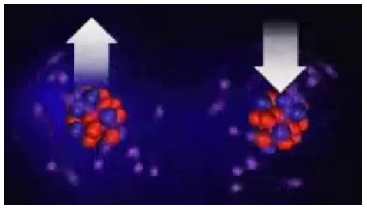

atom

**QUBIT**

(quantum mechanical)

$$|qubit\rangle = \frac{1}{\sqrt{2}}\left[\,|0\rangle + |1\rangle\,\right]$$

# Moore's Law

Moore:
The number of transistors on a chip doubles every $\sim$ two years

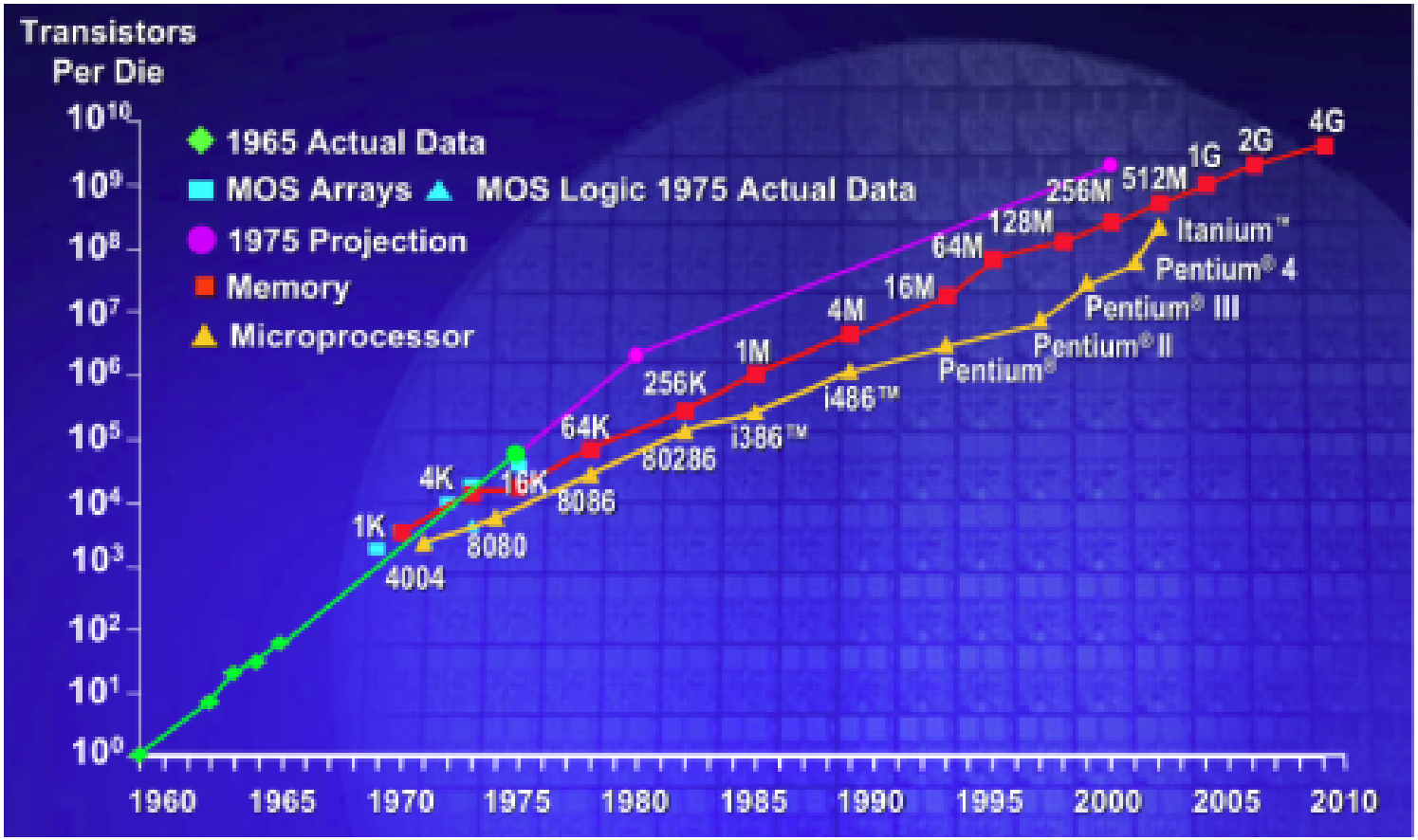

# Quantum Computer

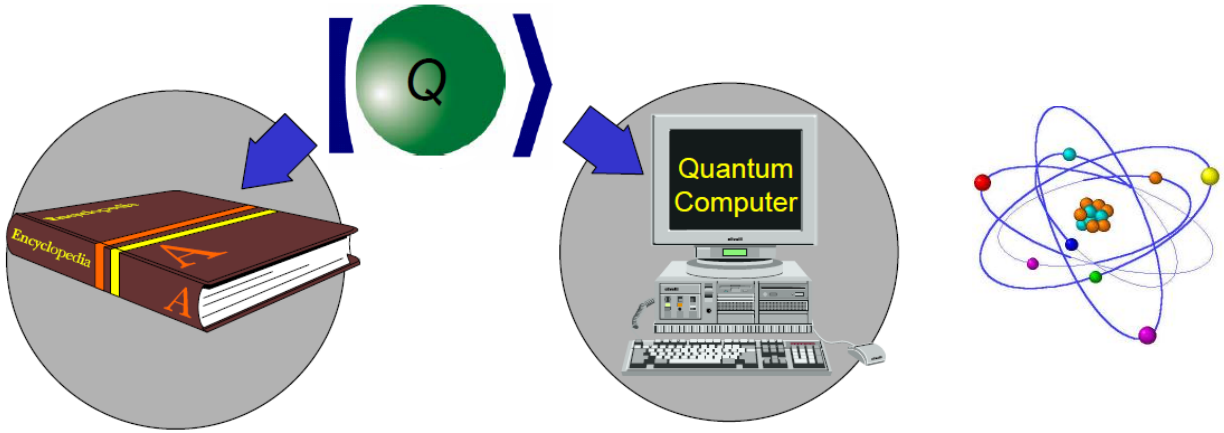


Quantum computer: (definition)

Video 01 ( 2 min. 24 sec.)

computer that makes direct use of quantum mechanical phenomena, such as

- superposition
- entanglement

that can perform tasks beyond the capability of any conceivable classical computer.

Molde University College
Specialized University in Logistics

# Applications of QC

- Faster calculations
- Perform detailed search more quickly
  - seach in a database
  - traveling salesman ( c.f. video )
- Simulate quantum mechanics better
  - chemistry and nanotechnology rely on understanding quantum system
  - simulate molecules for improvement of medical properties
- Quantum cryptography
  - credit cards
  - military secrets
  - Shor's algorithm (q. algorithm for integer factorization)
- lasers
- sensors

( Video 02 (2 min. 2 sec.) , Video 03 (1 min. 59 sec.) )

# Two Properties

Two peculiar properties:

- 1) superposition , mixture of all possible states
- 2) entanglement , “coupling” of quantum systems

# 1) Superposition

a) Classical computer: ($n = 3$ bits register, i.e. $2^n = 8$ alt.)

$$000\ ,\ 001\ ,\ 010\ ,011\ ,100\ ,\ 101\ ,\ 110\ ,111$$

b) Quantum computer:

$$|\psi\rangle_{in} = c_1|000\rangle + c_2|001\rangle + c_3|010\rangle + c_4|011\rangle$$
$$+c_5|100\rangle + c_6|101\rangle + c_7|110\rangle + c_8|111\rangle$$

where $\sum_{i=1}^{8} |c_i|^2 = 1$

Unitary operation: ( map )

$$|\psi\rangle_{out} = \hat{U}\,|\psi\rangle_{in}$$

$$= d_1|000\rangle + d_2|001\rangle + d_3|010\rangle + d_4|011\rangle + d_5|100\rangle + d_6|101\rangle + d_7|110\rangle + d_8|111\rangle$$

where $\sum_{i=1}^{8} |d_i|^2 = 1$

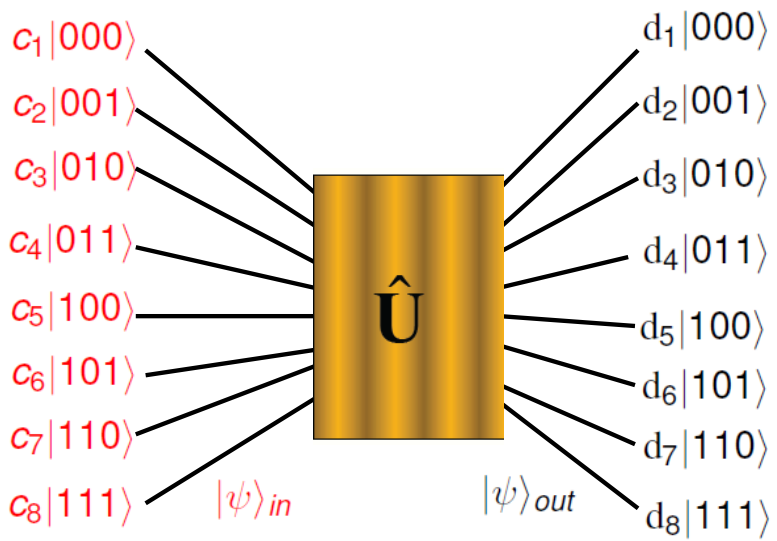


Molde University College
Specialized University in Logistics

Example:

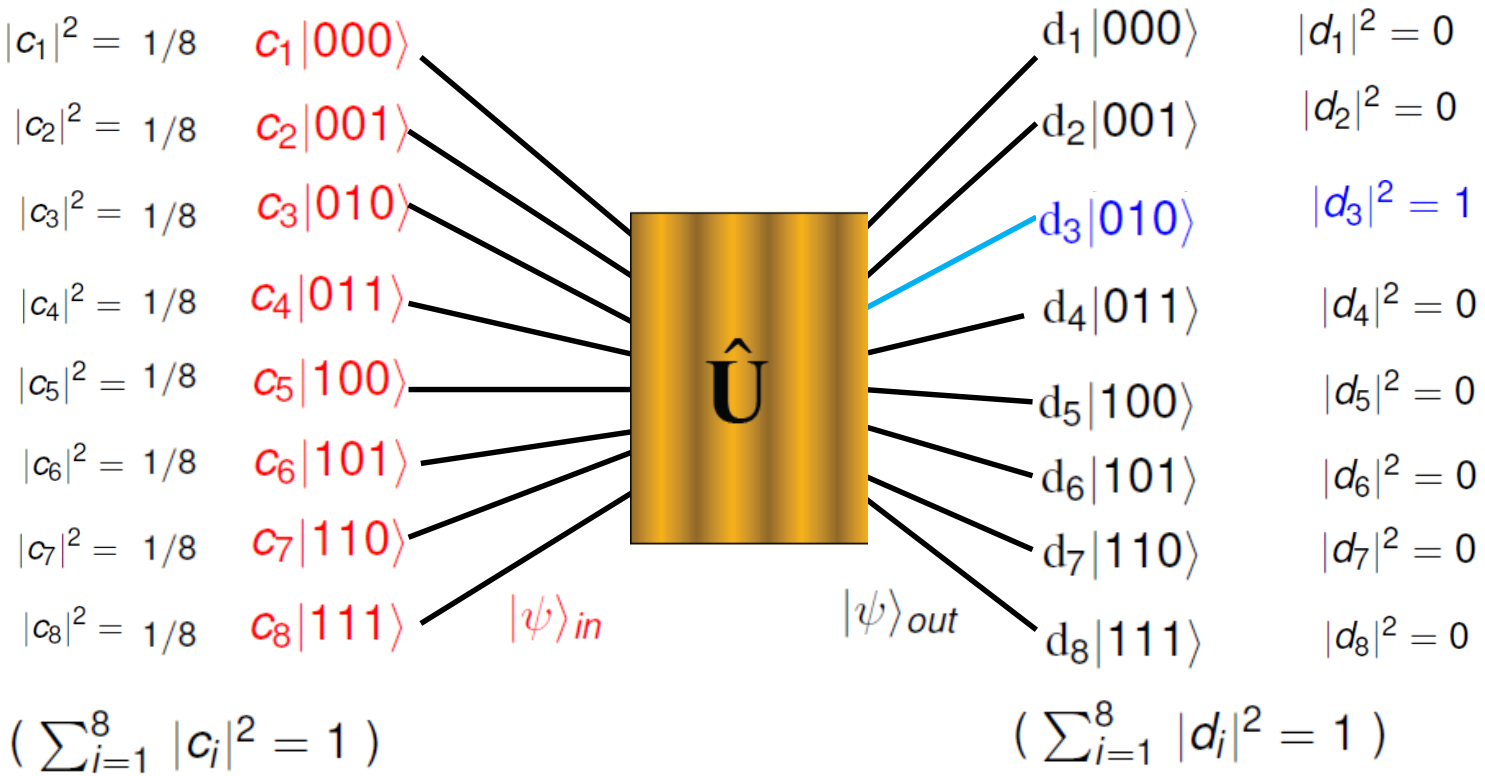


Molde University College
Specialized University in Logistics

# 1) Superposition (cont.)

Example:

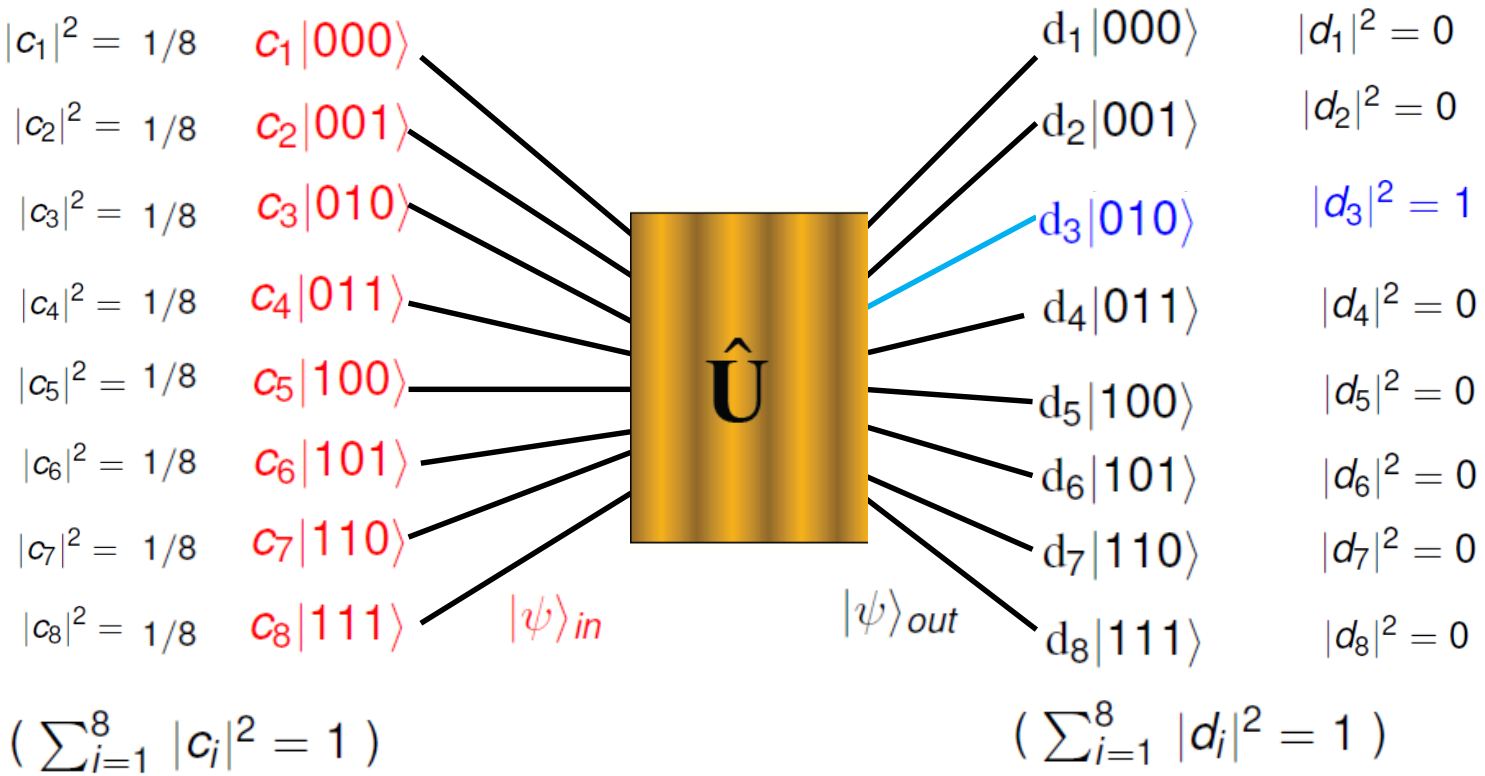


constructive / destructive interference

Molde University College
Specialized University in Logistics

# 2) Entanglement

Entanglement: (definition)

when two quantum systems interact and become irreversibly linked/coupled, or entangled.

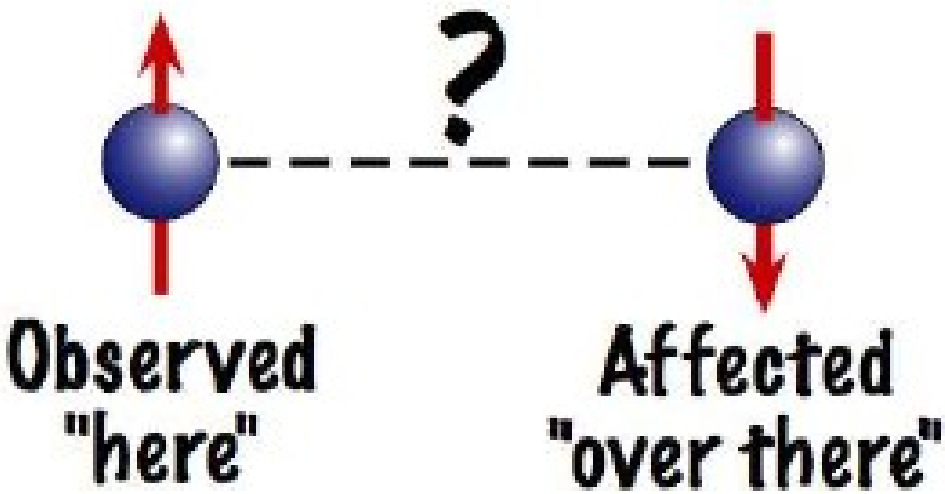


Video 04 (1 min. 2 sec.)

Molde University College
Specialized University in Logistics

# 2) Entanglement (cont.)

Einstein:

*“Spooky action at a distance”*

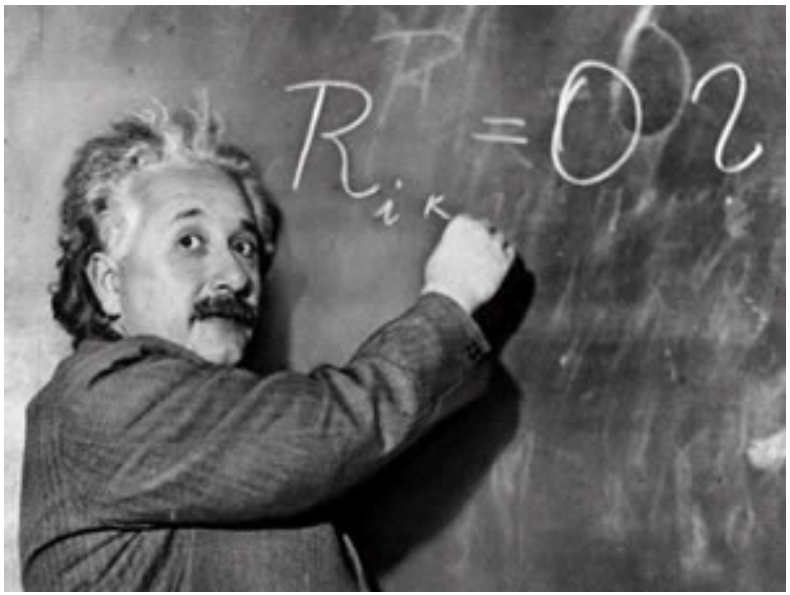


Molde University College
Specialized University in Logistics

New World Record

# New World Record


SCIENTIFIC AMERICAN™

SEARCH

- Log In or Register
- Log In to SA Digital

Energy & Sustainability | Evolution | Health | Mind & Brain | Space | Technology | More Sci

Home » Blogs » Observations »

**Observations**

Opinion, arguments & analyses from the editors of Scientific American

About *Observations* • RSS | More Blogs

## Physicists entangle a record-breaking 14 quantum bits

By John Matson | Apr 5, 2011 04:18 PM | 5

Share Email Print

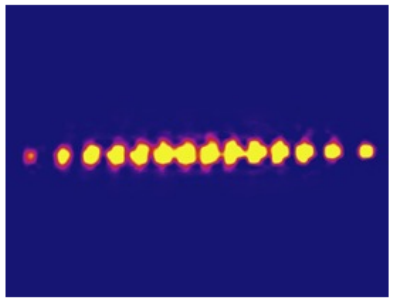

Quantum information science is a bit like classroom management—the larger the group, the harder it is to keep everything together.

But to build a practical quantum computer physicists will need many particles working in synchrony as quantum bits, or qubits. Each qubit can be a 0 and a 1 simultaneously, vaulting the number-crunching power of a hypothetical quantum computer well past that of ordinary computers. With each qubit in a superposition, a quantum computer can manipulate an exponentially large quantity of numbers at once—$2^n$ numbers for a system of $n$ qubits. So each step toward generating large sets of qubits pushes practical quantum computing closer to reality.

Molde University College
Specialized University in Logistics

Zoo of quantum optics systems

# Zoo of quantum optics systems

Ions in magnetic traps: ( quantum register )

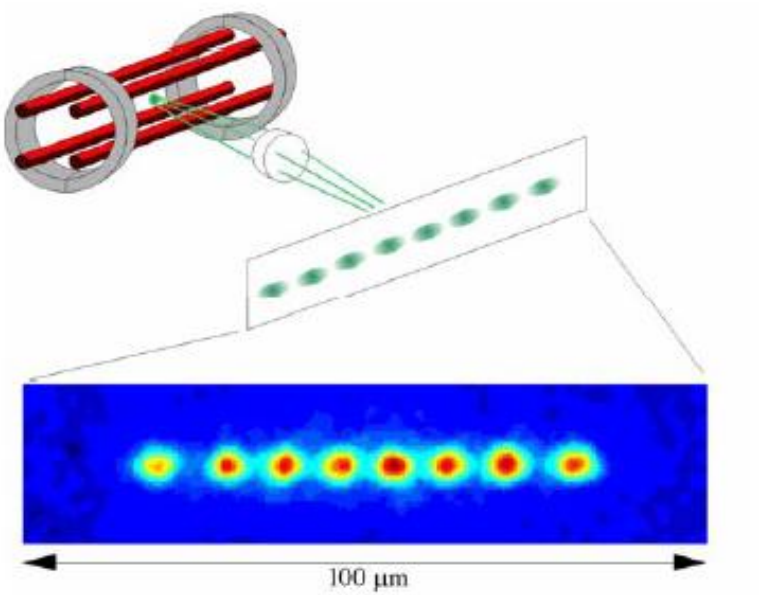


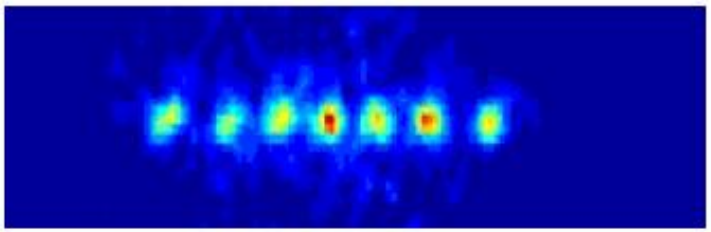

collective modes

Molde University College
Specialized University in Logistics

# Zoo of quantum optics systems (cont.)

Atoms trapped in a cavity: (atoms are qubits)

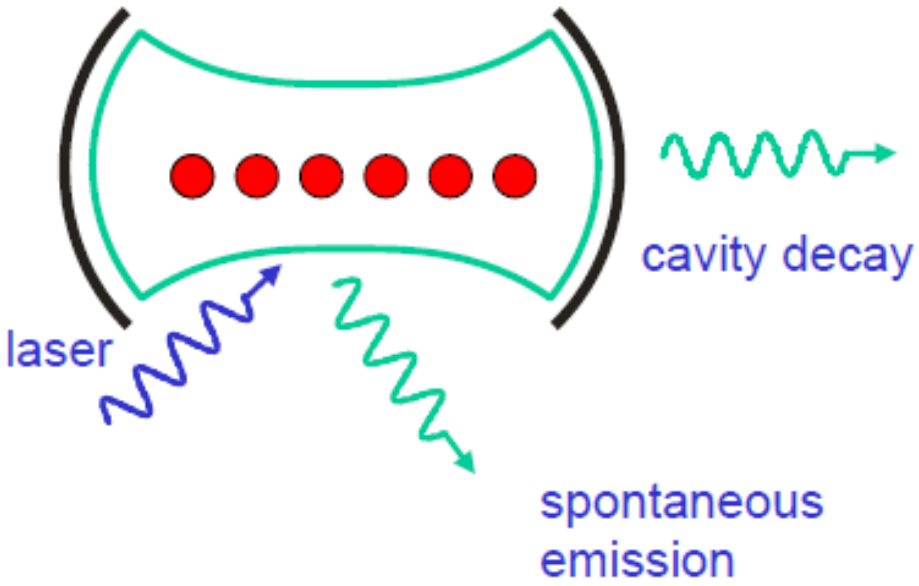


Molde University College
Specialized University in Logistics

# Zoo of quantum optics systems (cont.)

Optical lattice as array of microtraps for atoms:

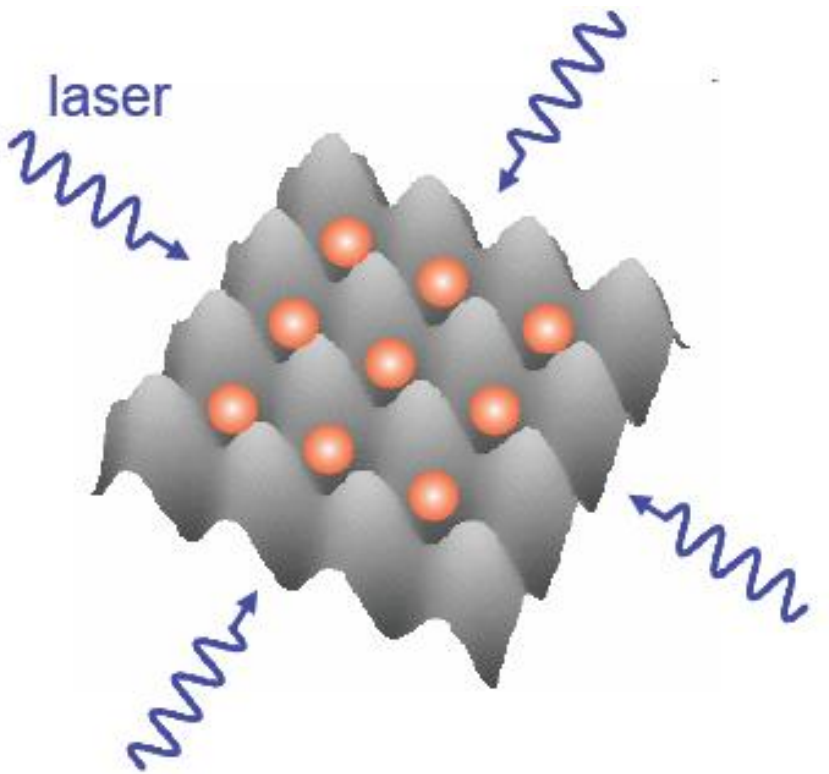


Molde University College
Specialized University in Logistics

# Decoherence

Decoherence

( loss of superposition , loss of ordering )

# Decoherence

PRL 97, 070401 (2006) PHYSICAL REVIEW LETTERS week ending 18 AUGUST 2006

## Spin Decoherence in Superconducting Atom Chips

Bo-Sture K. Skagerstam,[1,*] Ulrich Hohenester,[2] Asier Eiguren,[2] and Per Kristian Rekdal[2,†]

[1]*Complex Systems and Soft Materials Research Group, Department of Physics, The Norwegian University of Science and Technology, N-7491 Trondheim, Norway*

[2]*Institut für Physik, Karl-Franzens-Universität Graz, Universitätsplatz 5, A-8010 Graz, Austria*

(Received 25 March 2006; published 16 August 2006)

Using a consistent quantum-mechanical treatment for the electromagnetic radiation, we theoretically investigate the magnetic spin-flip scatterings of a neutral two-level atom trapped in the vicinity of a superconducting body. We derive a simple scaling law for the corresponding spin-flip lifetime for such an atom trapped near a superconducting thick slab. For temperatures below the superconducting transition temperature $T_c$, the lifetime is found to be enhanced by several orders of magnitude in comparison to the case of a normal conducting slab. At zero temperature the spin-flip lifetime is given by the unbounded free-space value.

DOI: 10.1103/PhysRevLett.97.070401 PACS numbers: 03.65.Yz, 03.75.Be, 34.50.Dy, 42.50.Ct

PRL 97, 070401 (2006) PHYSICAL REVIEW LETTERS week ending 18 AUGUST 2006

# Spin Decoherence in Superconducting Atom Chips

Bo-Sture K. Skagerstam,[1,*] Ulrich Hohenester,[2] Asier Eiguren,[2] and Per Kristian Rekdal[2,†]

[1]*Complex Systems and Soft Materials Research Group, Department of Physics, The Norwegian University of Science and Technology, N-7491 Trondheim, Norway*

[2]*Institut für Physik, Karl-Franzens-Universität Graz, Universitätsplatz 5, A-8010 Graz, Austria*

(Received 25 March 2006; published 16 August 2006)

Using a consistent quantum-mechanical treatment for the electromagnetic radiation, we theoretically investigate the magnetic spin-flip scatterings of a neutral two-level atom trapped in the vicinity of a superconducting body. We derive a simple scaling law for the corresponding spin-flip lifetime for such an atom trapped near a superconducting thick slab. For temperatures below the superconducting transition temperature $T_c$, the lifetime is found to be enhanced by several orders of magnitude in comparison to the case of a normal conducting slab. At zero temperature the spin-flip lifetime is given by the unbounded free-space value.

DOI: 10.1103/PhysRevLett.97.070401 PACS numbers: 03.65.Yz, 03.75.Be, 34.50.Dy, 42.50.Ct

Coherent manipulation of matter waves is one of the ultimate goals of atom optics. Trapping and manipulating cold neutral atoms in microtraps near surfaces of atomic chips is a promising approach towards full control of matter waves on small scales [1]. The subject of atom optics is making rapid progress, driven both by the fundamental interest in quantum systems and by the prospect of new devices based on quantum manipulations of neutral atoms.

With lithographic or other surface-patterning processes complex atom chips can be built which combine many traps, waveguides, and other elements, in order to realize controllable composite quantum systems [2] as needed, e.g., for the implementation of quantum information devices [3]. Such microstructured surfaces have been highly successful and form the basis of a growing number of experiments [4]. However, due to the proximity of the cold atom cloud to the macroscopic substrate additional decoherence channels are introduced which limit the performance of such atom chips. Most importantly, Johnson-noise currents in the material cause electromagnetic field fluctuations and hence threaten to decohere the quantum state of the atoms. This effect arises because the finite temperature and resistivity of the surface material are always accompanied by field fluctuations, as a consequence of the fluctuation-dissipation theorem. Several experimental [5–7] as well as theoretical [8–11] studies have recently shown that rf spin-flip transitions are the main source of decoherence for atoms situated close to metallic or dielectric bodies. Upon making spin-flip transitions, the atoms become more weakly trapped or even lost from the microtrap.

In Ref. [10] it was shown that to reduce the spin decoherence of atoms outside a metal in the normal state, one should avoid materials whose skin depth at the spin-flip transition frequency is comparable with the atom-surface distance. For typical values of these parameters used in experiments, however, this worst-case scenario occurs [5–7]. To overcome this deficiency, it was envisioned [9] that superconductors might be beneficial in this respect because of their efficient screening properties, although this conclusion was not backed by a proper theoretical analysis. It is the purpose of this letter to present a consistent theoretical description of atomic spin-flip transitions in the vicinity of superconducting bodies, using a proper quantum-mechanical treatment for the electromagnetic radiation, and to reexamine Johnson-noise induced decoherence for superconductors. We find that below the superconducting transition temperature $T_c$ the spin-flip lifetime becomes boosted by several orders of magnitude, a remarkable finding which is attributed to: (1) the opening of the superconducting gap and the resulting inability to deposit energy into the superconductor, (2) the highly efficient screening properties of superconductors, and (3) the small active volume within which current fluctuations can contribute to field fluctuations. Our results thus suggest that current-noise induced decoherence in atomic chips can be completely diminished by using superconductors instead of normal metals.

We begin by considering an atom in an initial state $|i\rangle$ and trapped at position $\mathbf{r}_A$ in vacuum, near a dielectric body. The rate of spontaneous and thermally stimulated magnetic spin-flip transition into a final state $|f\rangle$ has been derived in Ref. [10],

$$\Gamma^B = \mu_0 \frac{2(\mu_B g_S)^2}{\hbar} \sum_{j,k=1}^{3} \langle f|\hat{S}_j|i\rangle\langle i|\hat{S}_k|f\rangle \times \mathrm{Im}[\nabla \times \nabla \times \boldsymbol{G}(\mathbf{r}_A, \mathbf{r}_A, \omega)]_{jk}(\bar{n}_{\mathrm{th}} + 1). \quad (1)$$

Here $\mu_B$ is the Bohr magneton, $g_s \approx 2$ is the electron spin $g$ factor, $\langle f|\hat{S}_j|i\rangle$ is the matrix element of the electron spin operator corresponding to the transition $|i\rangle \to |f\rangle$, and $\boldsymbol{G}(\mathbf{r}_A, \mathbf{r}_A, \omega)$ is the dyadic Green tensor of Maxwell's theory. Equation (1) follows from a consistent quantum-mechanical treatment of electromagnetic radiation in the

 

presence of absorbing bodies [11,12]. Thermal excitations of the electromagnetic field modes are accounted for by the factor $(\bar{n}_{\rm th}+1)$, where $\bar{n}_{\rm th}=1/(e^{\hbar\omega/k_BT}-1)$ is the mean number of thermal photons per mode at frequency $\omega$ of the spin-flip transition. The dyadic Green tensor is the unique solution to the Helmholtz equation

$$\nabla\times\nabla\times\boldsymbol{G}(\mathbf{r},\mathbf{r}',\omega)-k^2\epsilon(\mathbf{r},\omega)\boldsymbol{G}(\mathbf{r},\mathbf{r}',\omega)=\delta(\mathbf{r}-\mathbf{r}')\mathbf{1}, \tag{2}$$

with appropriate boundary conditions. Here $k=\omega/c$ is the wave number in vacuum, $c$ is the speed of light and $\mathbf{1}$ the unit dyad. This quantity contains all relevant information about the geometry of the material and, through the electric permittivity $\epsilon(\mathbf{r},\omega)$, about its dielectric properties.

The current density in superconducting media is commonly described by the Mattis-Bardeen theory [13]. To simplify the physical picture, let us limit the discussion to low but nonzero frequencies $0<\omega\ll\omega_g\equiv 2\Delta(0)/\hbar$, where $\omega$ is the angular frequency and $\Delta(0)$ is the energy gap of the superconductor at zero temperature. In this limit, the current density is well described by means of a two-fluid model [14,15]. At finite temperature $T$, the current density consists of two types of carriers, superconducting Cooper pairs and normal conducting electrons. The total current density is equal to the sum of a superconducting current density and a normal conducting current density, i.e., $\mathbf{J}(\mathbf{r},t)=\mathbf{J}_s(\mathbf{r},t)+\mathbf{J}_n(\mathbf{r},t)$. Let us furthermore assume that the superconducting as well as the normal conducting part of the current density responds linearly and locally to the electric field [16], in which case the current densities are given by the London equation and Ohm's law, respectively,

$$\frac{\partial\mathbf{J}_s(\mathbf{r},t)}{\partial t}=\frac{\mathbf{E}(\mathbf{r},t)}{\mu_0\lambda_L^2(T)},\qquad \mathbf{J}_n(\mathbf{r},t)=\sigma_n(T)\mathbf{E}(\mathbf{r},t). \tag{3}$$

The London penetration length and the normal conductivity are given by,

$$\lambda_L^2(T)=\frac{m}{\mu_0 n_s(T)e^2},\qquad \sigma_n(T)=\frac{n_n(T)}{n_0}\sigma. \tag{4}$$

Here $\sigma$ is the electrical conductivity of the metal in the normal state, $m$ is the electron mass, $e$ is the electron charge, and $n_s(T)$ and $n_n(T)$ are the electron densities in the superconducting and normal state, respectively, at a given temperature $T$. Following London [14], we assume that the total density is constant and given by $n_0=n_s(T)+n_n(T)$, where $n_s(T)=n_0$ for $T=0$ and $n_n(T)=n_0$ for $T>T_c$. For a London superconductor with the assumptions as mentioned above, the dielectric function $\epsilon(\omega)$ in the low-frequency regime reads

$$\epsilon(\omega)=1-\frac{1}{k^2\lambda_L^2(T)}+i\frac{2}{k^2\delta^2(T)}, \tag{5}$$

where $\delta(T)\equiv\sqrt{2/\omega\mu_0\sigma_n(T)}$ is the skin depth associated with the normal conducting electrons. The optical conductivity corresponding to Eq. (5) is $\sigma(T)=2/\omega\mu_0\delta^2(T)+i/\omega\mu_0\lambda_L^2(T)$.

In the following we apply our model to the geometry shown in Fig. 1, where an atom is located in vacuum at a distance $z$ away from a superconducting slab. We consider, in correspondence to recent experiments [5–7], $^{87}$Rb atoms that are initially pumped into the $|5S_{1/2},F=2,m_F=2\rangle\equiv|2,2\rangle$ state. Fluctuations of the magnetic field may then cause the atoms to evolve into hyperfine sublevels with lower $m_F$. Upon making a spin-flip transition to the $m_F=1$ state, the atoms are more weakly trapped and are largely lost from the region of observation, causing the measured atom number to decay with rate $\Gamma_{21}^B$ associated with the rate-limiting transition $|2,2\rangle\rightarrow|2,1\rangle$. The transition rate $\Gamma_{21}^B=(\Gamma_{21}^0+\Gamma_{21}^{\rm slab})(\bar{n}_{\rm th}+1)$ can be decomposed into a free part and a part purely due to the presence of the slab. The free-space spin-flip rate at zero temperature is $\Gamma_{21}^0=\mu_0\frac{(\mu_B g_S)^2}{24\pi\hbar}k^3$ [10]. The slab-contribution can be obtained by matching the electromagnetic fields at the vacuum-superconductor interface. With the same spin orientation as in Ref. [9], i.e., $|\langle f|\hat{S}_y|i\rangle|^2=|\langle f|\hat{S}_z|i\rangle|^2$ and $\langle f|\hat{S}_x|i\rangle=0$, the spin-flip rate is $\Gamma_{21}^{\rm slab}=\Gamma_{21}^0(\tilde{I}_\parallel+\tilde{I}_\perp)$, with the atom-spin-orientation dependent integrals

$$\tilde{I}_\parallel=\frac{3}{8}\,{\rm Re}\Big(\int_0^\infty dq\,\frac{q}{\tilde{\eta}_0}e^{i2\tilde{\eta}_0kz}[r_p(q)-\tilde{\eta}_0^2r_s(q)]\Big), \tag{6}$$

$$\tilde{I}_\perp=\frac{3}{4}\,{\rm Re}\Big(\int_0^\infty dq\,\frac{q^3}{\tilde{\eta}_0}e^{i2\tilde{\eta}_0kz}r_s(q)\Big), \tag{7}$$

and the electromagnetic field polarization dependent Fresnel coefficients

$$r_s(q)=\frac{\tilde{\eta}_0-\tilde{\eta}(\omega)}{\tilde{\eta}_0+\tilde{\eta}(\omega)},\qquad r_p(q)=\frac{\epsilon(\omega)\tilde{\eta}_0-\tilde{\eta}(\omega)}{\epsilon(\omega)\tilde{\eta}_0+\tilde{\eta}(\omega)}. \tag{8}$$

Here we have $\tilde{\eta}(\omega)=\sqrt{\epsilon(\omega)-q^2}$ and $\tilde{\eta}_0=\sqrt{1-q^2}$. In

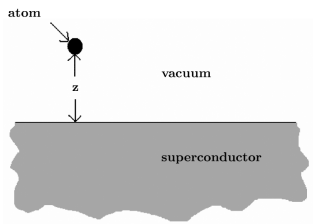


FIG. 1. Schematic picture of the setup considered in our calculations. An atom inside a magnetic microtrap is located in vacuum at a distance $z$ away from a thick superconducting slab, i.e., a semi-infinite plane. Upon making a spin-flip transition, the atom becomes more weakly trapped and is eventually lost.

particular, above the transition temperature $T_c$ the dielectric function in Eq. (5) reduces to the well-known Drude form. Because of the efficient screening properties of superconductors, in most cases of interest the inequality $\lambda_L(T) \ll \delta(T)$ holds. Assuming furthermore the near-field case $\lambda_L(T) \ll z \ll \lambda$, where $\lambda = 2\pi/k$ is the wavelength associated to the spin-flip transition, which holds true in practically all cases of interest, we can compute the integrals in Eqs. (6)–(8) analytically to finally obtain

$$\Gamma_{21}^{B} \approx \Gamma_{21}^{0}(\bar{n}_{\mathrm{th}} + 1)\left[1 + 2\left(\frac{3}{4}\right)^{3} \frac{1}{k^3 \delta(T)^2} \frac{\lambda_L^3(T)}{z^4}\right]. \quad (9)$$

For a superconductor at $T = 0$, in which case there are no normal conducting electrons, it is seen from Eq. (9) that the lifetime is given by the unbounded free-space lifetime $\tau_0 \equiv 1/\Gamma_{21}^{0}$.

Equation (9) is the central result of our Letter. To inquire into its details, we compute the spin-flip rate for the superconductor niobium (Nb) and for a typical atomic transition frequency $\nu \equiv \omega/2\pi = 560$ kHz [5]. We keep the atom-surface distance fixed at $z = 50$ $\mu$m, and use the Gorter-Casimir [15] temperature dependence

$$\frac{n_s(T)}{n_0} = 1 - \frac{n_n(T)}{n_0} = 1 - \left(\frac{T}{T_c}\right)^4, \quad (10)$$

for the superconducting electron density. Figure 2 shows the spin-flip lifetime $\tau_s \equiv 1/\Gamma_{21}^{B}$ of the atom as a function of temperature: over a wide temperature range $\tau_s$ remains as large as $10^{10}$ sec. In comparison to the normal-metal lifetime $\tau_n$, which is obtained for aluminum with its quite small skin depth $\delta = 110$ $\mu$m and using the results of Refs. [9,10], we observe that the lifetime becomes boosted by almost 10 orders of magnitude in the superconducting state. In particular, for $T = 0$ the ratio between $\tau_s$ and $\tau_n$ is even $10^{17}$. From the scaling behavior Eq. (9) we thus observe that decoherence induced by current fluctuations in the superconducting state remains completely negligible even for small atom-surface distances around 1 $\mu$m, in strong contrast to the normal state where such decoherence would limit the performance of atomic chips.

The scaling behavior of the spin-flip rate Eq. (9) can be understood qualitatively on the basis of Eq. (1). The fluctuation-dissipation theorem [11,12] relates the imaginary part of the Green tensor and $\epsilon(\omega)$ by $\mathrm{Im}\mathbf{G} = \mathbf{G}\,\mathrm{Im}[\epsilon(\omega)]\mathbf{G}^{*}$, assuming a suitable real-space convolution, and allows to bring the scattering rate Eq. (1) to a form reminiscent of Fermi's golden rule. The magnetic dipole of the atom at $\mathbf{r}_A$ couples to a current fluctuation at point $\mathbf{r}$ in the superconductor through $\boldsymbol{G}(\mathbf{r}_A, \mathbf{r}, \omega)$. The propagation of the current fluctuation is described by the dielectric function $\epsilon(\omega)$, and finally a backaction on the atomic dipole occurs via $\boldsymbol{G}(\mathbf{r}, \mathbf{r}_A, \omega)$. For the near-field coupling under consideration, $z \ll \lambda$, the dominant contribution of the Green tensor is $|\mathbf{G}| \sim 1/z^2$, thus resulting in the overall $z^{-4}$ dependence of the spin-flip rate Eq. (9).

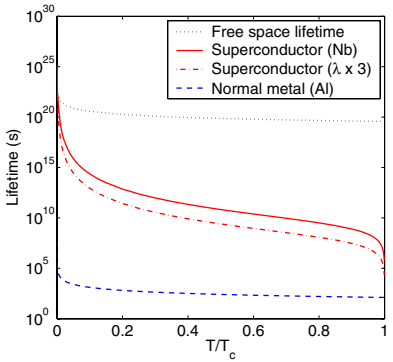


FIG. 2 (color online). Spin-flip lifetime of a trapped atom near a superconducting slab $\tau_s$ (red solid line) as a function of temperature $T$. The atom-surface distance is fixed at $z = 50$ $\mu$m, and the frequency of the atomic transition is $\nu = 560$ kHz. The other parameters are $\lambda_L(0) = 35$ nm [19], $\sigma \approx 2 \times 10^9$ $(\Omega\,\mathrm{m})^{-1}$ [20], and $T_c = 8.31$ K [19], corresponding to superconducting Nb. The numerical value of $\tau_s$ is computed using the temperature dependence as given by Eq. (10). As a reference, we have also plotted the lifetime $\tau_n$ (blue dashed line) for an atom outside a normal conducting slab with $\delta = 110$ $\mu$m, corresponding to Al. The red dashed-dotted line is the lifetime for the same parameters as mentioned above but $\lambda_L(0) = 3 \times 35$ nm, i.e., where we have taken into account the fact that the London length is modified due to nonlocal effects. The dotted line corresponds to the lifetime $\tau_0/(\bar{n}_{\mathrm{th}} + 1)$ for a perfect normal conductor. The unbounded free-space lifetime at zero temperature is $\tau_0 \approx 10^{25}$ s.

The imaginary part $\mathrm{Im}[\epsilon(\omega)] \sim 1/\delta^2$ of the dielectric function Eq. (5) accounts for the loss of electromagnetic energy to the superconductor, and is only governed by electrons in the normal state, whereas electrons in the superconducting state cannot absorb energy because of the superconducting gap. Finally, the term $\lambda^3$ is due to the dielectric screening $1/\epsilon(\omega) \sim \lambda^2$ of the charge fluctuation seen by the atom, and an additional $\lambda$ contribution associated to the active volume of current fluctuations which contribute to the magnetic field fluctuations at the position of the atom. Fluctuations deeper inside the superconductor are completely screened out. In comparison to the corresponding scaling $\Gamma^{B} \sim \delta/z^4$ for a normal metal [9], which can be qualitatively understood by a similar reasoning, the drastic lifetime enhancement in the superconducting state is thus due to the combined effects of the opening of the superconducting gap, the highly efficient screening, and the small active volume.

Let us finally briefly comment on the validity of our simplified approach, and how our results would be modi-

fied if using a more refined theory for the description of the superconductor. Our theoretical approach is valid in the same parameter regime as London's theory, that is $\lambda(T) \gg \xi(T)$. It is well known that nonlocal effects modify the London length in Nb from $\lambda_L(0) \approx 35$ nm to $\lambda(0) \approx 90$ nm [17], and the coherence length $\xi(T)$, according to Pippard's theory [18], from the BCS value $\xi_0$ to $1/\xi(T) = 1/\xi_0 + 1/\alpha\ell(T)$, where $\alpha$ is of the order one and $l(T)$ is the mean free path. For Nb, $\xi_0 = 39$ nm and $l(T \leq 9\ \mathrm{K}) \cong 9$ nm [19], and the London condition $\lambda(T) \gg \xi(T)$ is thus satisfied. Furthermore, at the atomic transition frequency the conductivity is $\sigma \approx 2 \times 10^9\ (\Omega\,\mathrm{m})^{-1}$ [20] and the corresponding skin depth is $\delta = \sqrt{2/\omega\mu_0\sigma} \approx 15\ \mu\mathrm{m} \leq \delta(T)$, such that Ohm's law is also valid since $\delta(T) \gg l(T)$ [21]. It is important to realize that other possible modifications of the parameters used in our calculations, as, e.g., a modification of Eq. (10) for $T/T_c \lesssim 0.5$ [22,23] will by no means drastically change our findings, which only rely on the generic superconductor properties of the efficient screening and the opening of the energy gap, and that our conclusions will also prevail for other superconductor materials.

We also mention that for both a superconductor at $T = 0$ and a perfect normal conductor, i.e. $\delta = 0$, the lifetime is given by the unbounded free-space lifetime $\tau_0$. In passing, we notice that for an electric dipole transition and for a perfect normal conductor, as, e.g., discussed in Refs. [24], the correction to the vacuum rate is in general opposite in sign as compared to that of a magnetic dipole transition. Elsewhere decay processes in the vicinity of a thin superconducting film will be discussed in detail [25].

To summarize, we have used a consistent quantum theoretical description of the magnetic spin-flip scatterings of a neutral two-level atom trapped in the vicinity of a superconducting body. We have derived a simple scaling law for the corresponding spin-flip lifetime for a superconducting thick slab. For temperatures below the superconducting transition temperature $T_c$, the lifetime has been found to be enhanced by several orders of magnitude in comparison to the case of a normal conducting slab. We believe that this result represents an important step towards the design of atomic chips for high-quality quantum information processing.

We are grateful to Heinz Krenn for helpful discussions. This work has been supported in part by the Austrian Science Fund (FWF).

*Electronic address: boskag@phys.ntnu.no
†Electronic address: per.rekdal@uni-graz.at

[1] R. Folman, P. Krüger, J. Schmiedmayer, J. Denschlag, and C. Henkel, Adv. At. Mol. Opt. Phys. **48**, 263 (2002).
[2] P. Zoller, Nature (London) **404**, 236 (2002).
[3] D. P. DiVincenzo, Fortschr. Phys. **48**, 771 (2000).
[4] P. Hommelhoff, W. Häsel, T. W. Hänsch, and J. Reichel New J. Phys. **7**, 3 (2005).
[5] M. P. A. Jones, C. J. Vale, D. Sahagun, B. V. Hall, and E. A. Hinds, Phys. Rev. Lett. **91**, 080401 (2003).
[6] Y. J. Lin, I. Teper, C. Chin, and V. Vuletic, Phys. Rev. Lett. **92**, 050404 (2004).
[7] D. M. Harber, J. M. McGuirk, J. M. Obrecht, and E. A. Cornell, J. Low Temp. Phys. **133**, 229 (2003).
[8] C. Henkel, S. Pötting, and M. Wilkens, Appl. Phys. B **69**, 379 (1999); C. Henkel and M. Wilkens, Europhys. Lett. **47**, 414 (1999).
[9] S. Scheel, P. K. Rekdal, P. L. Knight, and E. A. Hinds, Phys. Rev. A **72**, 042901 (2005).
[10] P. K. Rekdal, S. Scheel, P. L. Knight, and E. A. Hinds, Phys. Rev. A **70**, 013811 (2004).
[11] L. Knöll, S. Scheel, and D.-G. Welsch, in *Coherence and Statistics of Photons and Atoms*, edited by J. Peřina (Wiley, New York, 2001); T. D. Ho Trung Dung, L. Knöll, and D.-G. Welsch, Phys. Rev. A **62**, 053804 (2000); S. Scheel, L. Knöll, and D.-G. Welsch, Phys. Rev. A **60**, 4094 (1999); S. Scheel, L. Knöll, and D.-G. Welsch, Phys. Rev. A **60**, 1590 (1999).
[12] C. Henry and R. Kazarinov, Rev. Mod. Phys. **68**, 801 (1996).
[13] D. C. Mattis and J. Bardeen, Phys. Rev. **111**, 412 (1958).
[14] H. London, Nature (London) **133**, 497 (1934); H. London, Proc. R. Soc. A **176**, 522 (1940).
[15] C. S. Gorter and H. Casimir, Z. Phys. **35**, 963 (1934); Z. Tech. Phys. **15**, 539 (1934); C. J. Gorter, in *Progress in Low Temperature Physics* (North-Holland, Amsterdam, 1955).
[16] Strictly speaking, a local dielectric response is only valid if, for a given temperature $T$, the skin depth $\delta(T)$ associated with the normal conducting part of the current density is sufficiently large in comparison to the mean free path $l(T)$ of the electrons and the penetration depth $\lambda(T)$ of the field large in comparison to the superconductor coherence length $\xi(T)$. Superconductors satisfying the latter condition are known as London superconductors.
[17] P. B. Miller, Phys. Rev. **113**, 1209 (1959).
[18] A. B. Pippard, Proc. R. Soc. A **216**, 547 (1953).
[19] A. V. Pronin, M. Dressel, A. Primenov, and A. Loidl, Phys. Rev. B **57**, 14 416 (1998).
[20] S. Casalbuoni, E. A. Knabbe, J. Kötzler, L. Lilje, L. von Sawilski, P. Schmüser, and B. Steffen, Nucl. Instrum. Methods Phys. Res., Sect. A **538**, 45 (2005).
[21] G. E. H. Reuter and E. H. Sondheimer, Proc. R. Soc. A **195**, 336 (1948).
[22] J. G. Daunt, A. R. Miller, A. B. Pippard, and D. Shoenberg, Phys. Rev. **74**, 842 (1948).
[23] J. P. Turneaure, J. Halbitter, and H. A. Schwettman, J. Supercond. **4**, 341 (1991).
[24] P. W. Milonni and P. L. Knight, Opt. Commun. **9**, 119 (1973); G. S. Agarwal, Phys. Rev. A **11**, 230 (1975); M. Babiker, J. Phys. A **9**, 799 (1976).
[25] P. K. Rekdal and B.-S. Skagerstam (unpublished).

# Lifetime of an Atom Chip

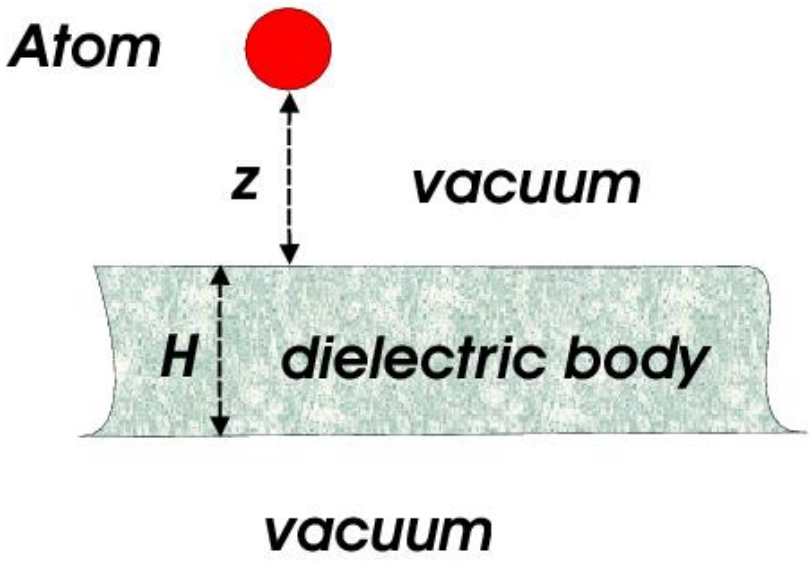

# Lifetime of an Atom Chip

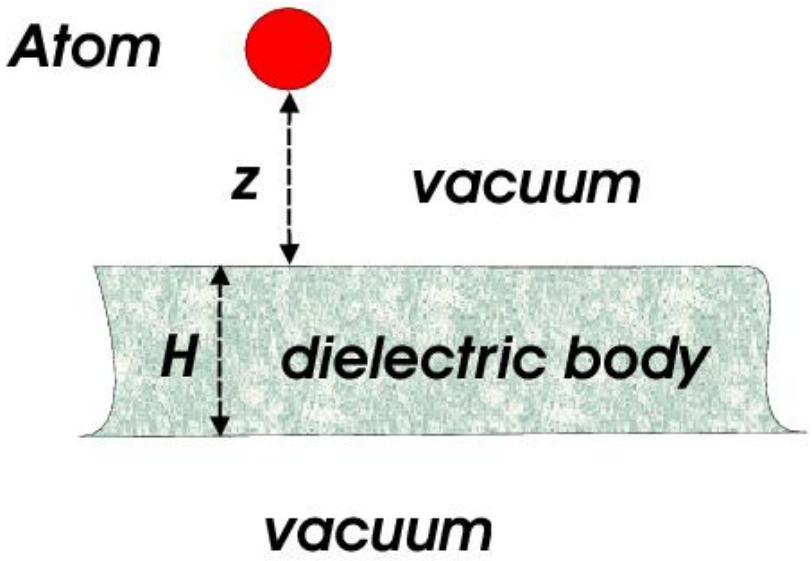


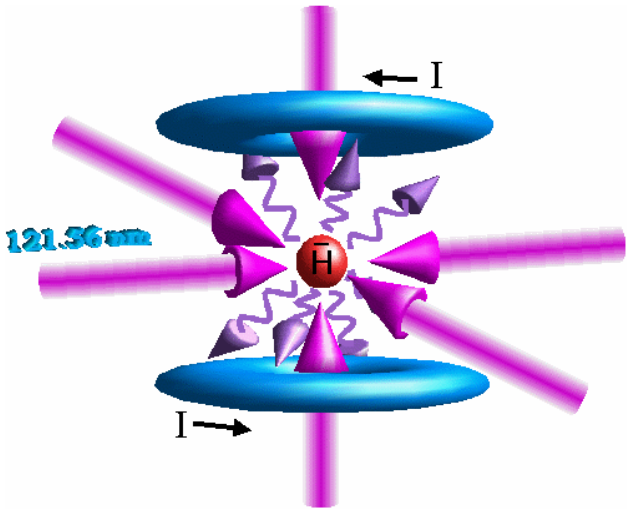


Molde University College
Specialized University in Logistics

# Lifetime of an Atom Chip

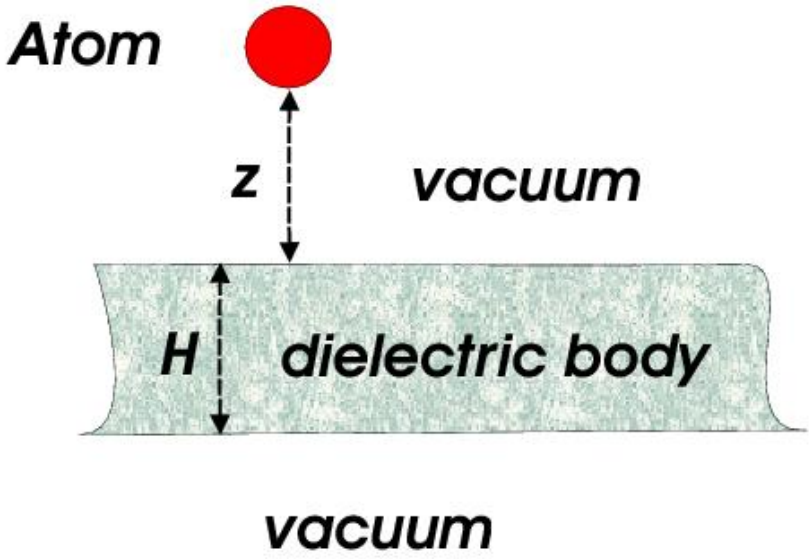


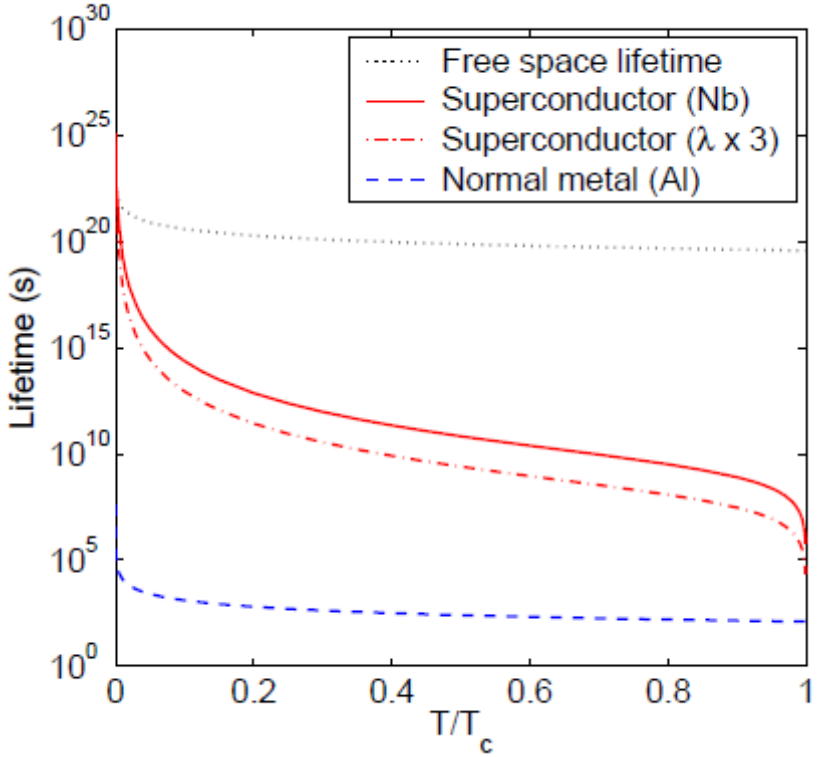


Molde University College
Specialized University in Logistics

# Collaborators

Currently am I working with the following persons:

Prof. Bo-Sture Skagerstam, NTNU

Asle Heide Vaskinn, Ph. D. student, NTNU

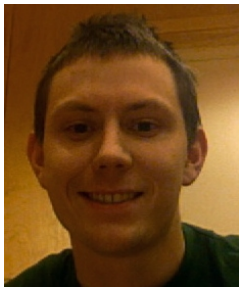

Arne Løhre Grimsmo, Ph. D. student, NTNU

# Summary

- My research concerns:
  - theoretical physics
  - quantum optics (QO)


- Possible applications of QO:
  - chemistry, nanotechnology, sensors and lasers
  - simulate molecules for improvement of medical properties
  - quantum computers, quantum cryptography
- Possible practical application for hiMolde:
  - research project, sensor technique for real time monitoring
    - research project funded by "RFF Midt-Norge"?
    - collaboration with offshore enginnering companies in Molde?
- My next 3 years at hiMolde
  - 1) research and publication at hiMolde ("level 2")
  - 2) research collaboration with groups at hiMolde
  - 3) teaching